4-7 Assaying

The equipment of fluorescent X-ray analysis functioned normally.

For the 5 elements: Ni, Cu, Co, Mn and Fe that are principal components of the collected manganese nodules, the fluorescent X-ray analysis was executed on board.

The number of the analyzed samples was as follows:

- manganese nodules: 190
- manganese nodule sections: 26
- bottom materials: 8

Also, for the purpose of inspection on the bias, 50 samples were used for the wet chemical analysis (analysis on shore).

The results of inspection on bias and accidental errors are described below:

1) Inspection on the bias

Scatter diagram of metal grade assayed on board and on shore showed distinct linear distribution, and regression coefficient estimated by the diagram was nearly 1.

Therefore, inspection on the bias and accidental errors was examined by means of regression analysis considering the results of Inspection on the difference of average values by means of t-test.

The following are the upper and lower value of the calibration curve.

Metal	Upper grade	Lower grade	Number of samples
Ni	1.69%	0.05%	23
Cu	1.53	0.05	22
Co	0.63	0.02	19
Mn	33.77	2.62	22
Fe	18.33	1.76	21

(1) Method by regression analysis

The regression equation: $Y = aX + b$ was utilised.

Y: value of the wet chemical analysis

X: fluorescent X-ray analysis on board

a: regression coefficient

b: constant term

The results of the t-test relating to the estimated values of a and b of the regression equation and to the values of regression coefficient are shown in Table 4-7-1.

Further, the correlation coefficients between the analysis values on board and the chemical analysis values are given together. The estimated values of bias and accidental errors are also shown in Table 4-7-2.

(2) Test on the difference of average values

Table 4-7-3 shows the estimated values of bias and accidental errors obtained from the results of the t-test on the difference between respective mean values of the analysis on board and the chemical analysis.

2) Examination of the results

As shown in Table 4-7-1, it could be considered that the analysis values on board and those t-tested ashore had completely a full correlationship.

Table 4-7-1 Estimated Values of a, b and Correlation Coefficients

	a	b	t calculated	t	Correlation coefficient
Ni	1.0897	−0.0231	2.3863	2.686	0.9726
Cu	0.9594	0.0459	1.1753	//	0.9703
Co	1.0666	0.0370	1.4617	//	0.9589
Mn	1.0634	−1.4762	4.1436	//	0.9951
Fe	1.0455	−0.0069	2.1125	//	0.9900

t degree of freedom: 4 and 5, significant level ±1%

Table 4-7-2 Examination of the bias and the accidental errors by Regression analysis

	Average grade assayed on board	Bias estimated	Accidental error estimated	Relative bias
Ni	0.300% 1.100%	0.004% 0.076%	± 0.044% ± 0.058%	1 % 7 %
Cu	0.200% 0.800%	0.038% 0.013%	± 0.030% ± 0.043%	19 % 2 %
Co	0.200% 0.400%	0.050% 0.064%	± 0.013% ± 0.024%	25 % 16 %
Mn	7.000% 24.000%	−1.033% 0.045%	± 0.466% ± 0.396%	−15 % 0.2%
Fe	7.000% 16.000%	0.311% 0.720%	± 0.286% ± 0.374%	4 % 5 %

Table 4-7-3 Bias and Accidental Errors Resulting from Inspection of the Difference of Average Values

	Average grade assayed on board	Bias estimated	Accidental error estimated	Relative bias	t calculated	t
Ni	0.6466 %	0.032 %	± 0.032 %	5 %	2.696	2.686
Cu	0.4360 %	0.029 %	± 0.023 %	7 %	3.394	//
Co	0.2830 %	0.052 %	± 0.013 %	18 %	10.930	//
Mn	16.1280 %	− 0.427 %	± 0.290 %	3 %	3.949	//
Fe	11.0042 %	0.472 %	± 0.207 %	4 %	6.112	//

t degree of freedom: 4 and 5, significant level ±1%

Accidental error of the data assayed on board means provability 95%

This is easily concluded for the reason that even though a slight difference is observed on the regression coefficients and constant terms of each element, the both values of analysis in the dispersion figure are distributed along a straight line for each element and all the regression coefficients are close to 1.

Then, examining the bias by the difference of mean values, the bias presents rather higher values related to the cobalt than in case of the regression analysis. However, the bias related to each component could be estimated not to be so large as to make inconvenience practically.

4-8 Manganese Nodules

Sampling of manganese nodules using FG and SC was done at a total of 114 sampling points (38 stations).

The sample manganese nodules were measured and observed in many different ways on the vessel.

On shore, chemical and mineral analysis was performed on some representative samples.

1) Physical properties (Morphology and granular size - characteristics by external appearance - water content and specific gravity)

(1) Morphology

Classification of manganese nodule morphology is 7 as follows:

① spheroidal type

② ellipsoidal type

③ ellipsoidal fat type

④ pebble thin type

⑤ massive type

⑥ plate type

⑦ other type

General explanations about each manganese nodule morphology is as follows. Tab. 4-8-1 shows physical properties of each morphology.

① Spheroidal type (cf. Fig. 4-8-1)

There are two types: small size (0 - 4 cm) and medium size (more than 4 cm). The small size type mainly has a rough and proturberant surface like a cedar sphere nut, and often has a smooth surface. The medium size type is charcoal nugget shaped and slightly brown with a coarse granular surface.

② Ellipsoidal type (cf. Fig. 4-8-1)

This type has a hamburger like outward form with a fine irregular and rough surface and is mainly manganese nodules with small cracks. Manganese nodules in the surveyed areas are mainly small and have unknown thickness with a fragmented coating.

③ Ellipsoidal fat type (cf. Fig. 4-8-2)

This type is one of the variations of the medium spheroidal type and is more irregular and larger than ellipsoidal type which appears most often in the surveyed areas.

④ Pebble thin type (cf. Fig. 4-8-2)

This type is usually a small manganese nodules with a thin and round or oval shape like small stones on the seashore or like "igo" stonesand with a relatively smooth surface without irregularity.

⑤ Massive type (cf. Fig. 4-8-3)

This type has a relatively smooth surface with irregular angularity and a thin plate shape varying between the small and large size.

Table 4-8-1 Physical Properties Associated with Morphology of Manganese Nodules

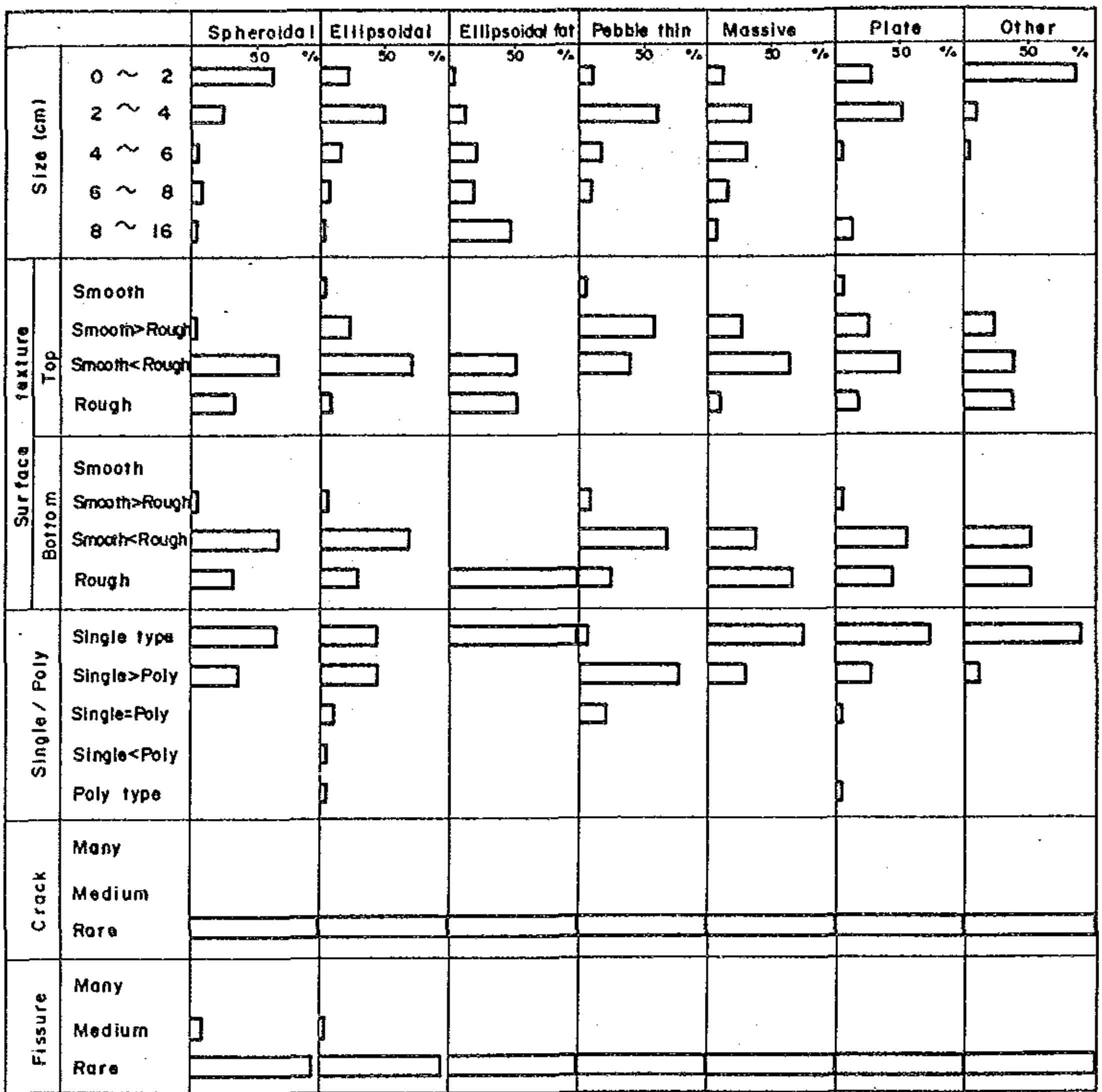

		Spheroidal	Ellipsoidal	Ellipsoidal fat	Pebble thin	Massive	Plate	Other
Moisture content(%)	Mean	26.60	27.65	31.66	26.84	26.28	28.56	18.46
	Standard deviation	3.16	3.35	4.02	2.42	6.61	5.14	1.73
	Maximum	37.37	35.19	36.70	32.04	34.78	37.50	20.34
	Minimum	20.46	20.00	28.28	22.64	7.50	13.89	16.28
Specific gravity(wet)	Mean	2.05	2.04	1.96	2.01	2.05	1.98	2.10
	Standard deviation	0.07	0.08	0.11	0.07	0.15	0.12	0.08
	Maximum	2.23	2.27	2.12	2.15	2.49	2.27	2.20
	Minimum	1.90	1.87	1.89	1.84	1.87	1.79	2.00

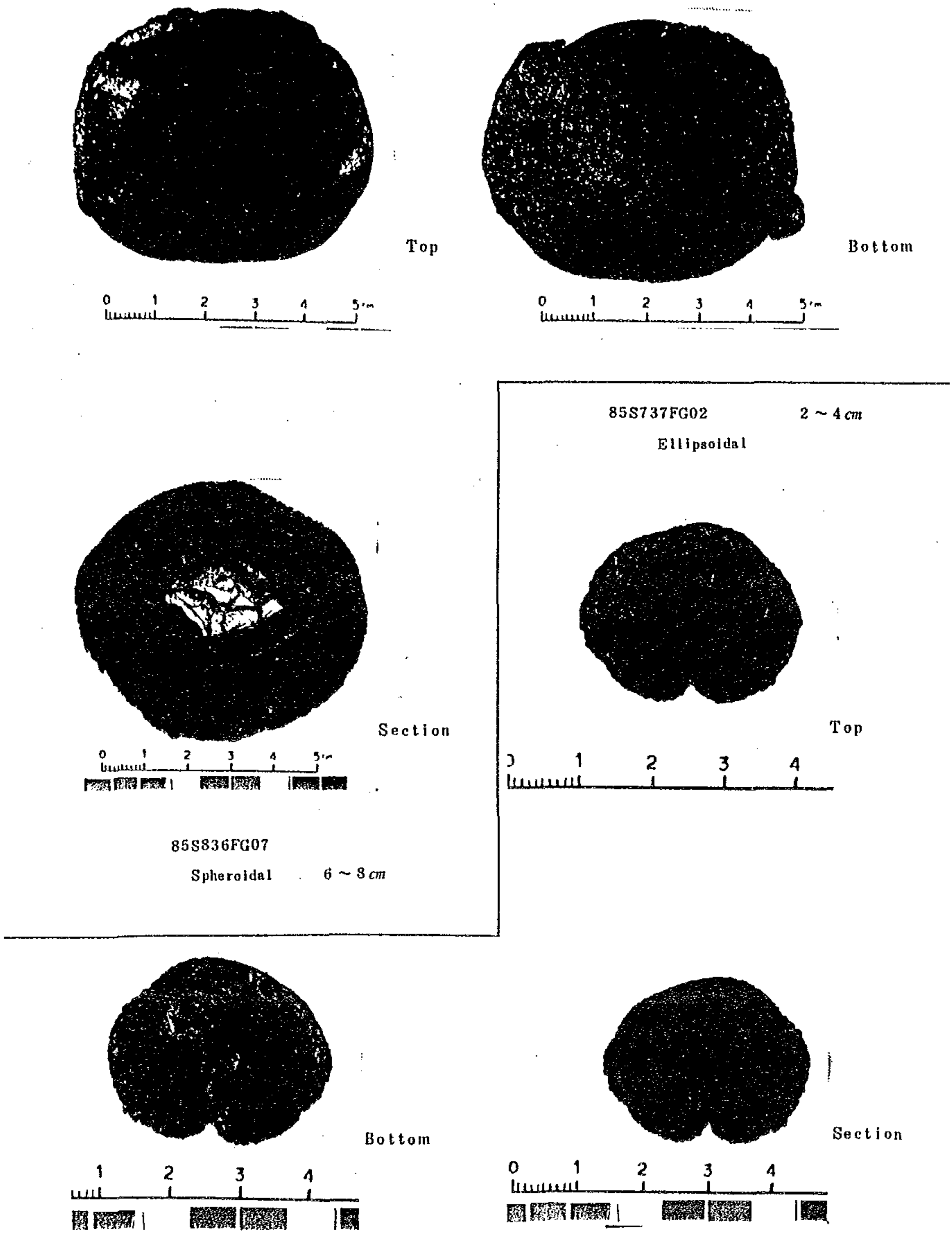

Fig. 4-8-1 Morphology of Manganese Nodules (No.1)

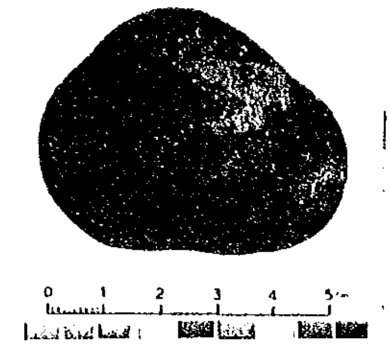

Top

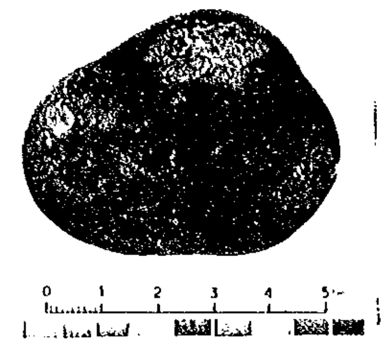

Bottom

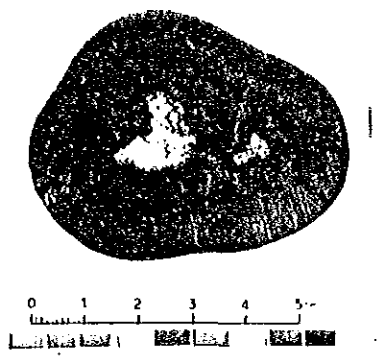

Section

85S936FG02 4 ~ 6 *cm*
Ellipsoidal fat

85S739FG03 2 ~ 4 *cm*
Pebble thin

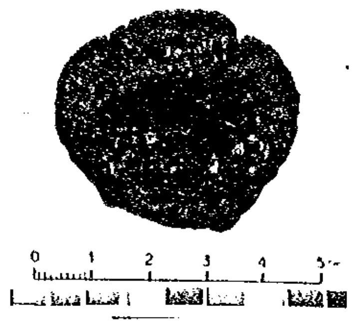

Top

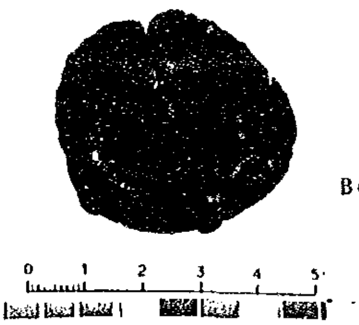

Bottom

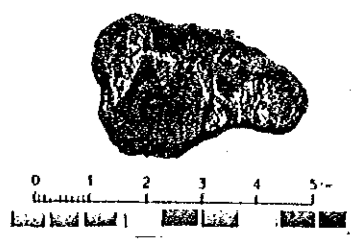

Section

Fig. 4-8-2 Morphology of Manganese Nodules (No.2)

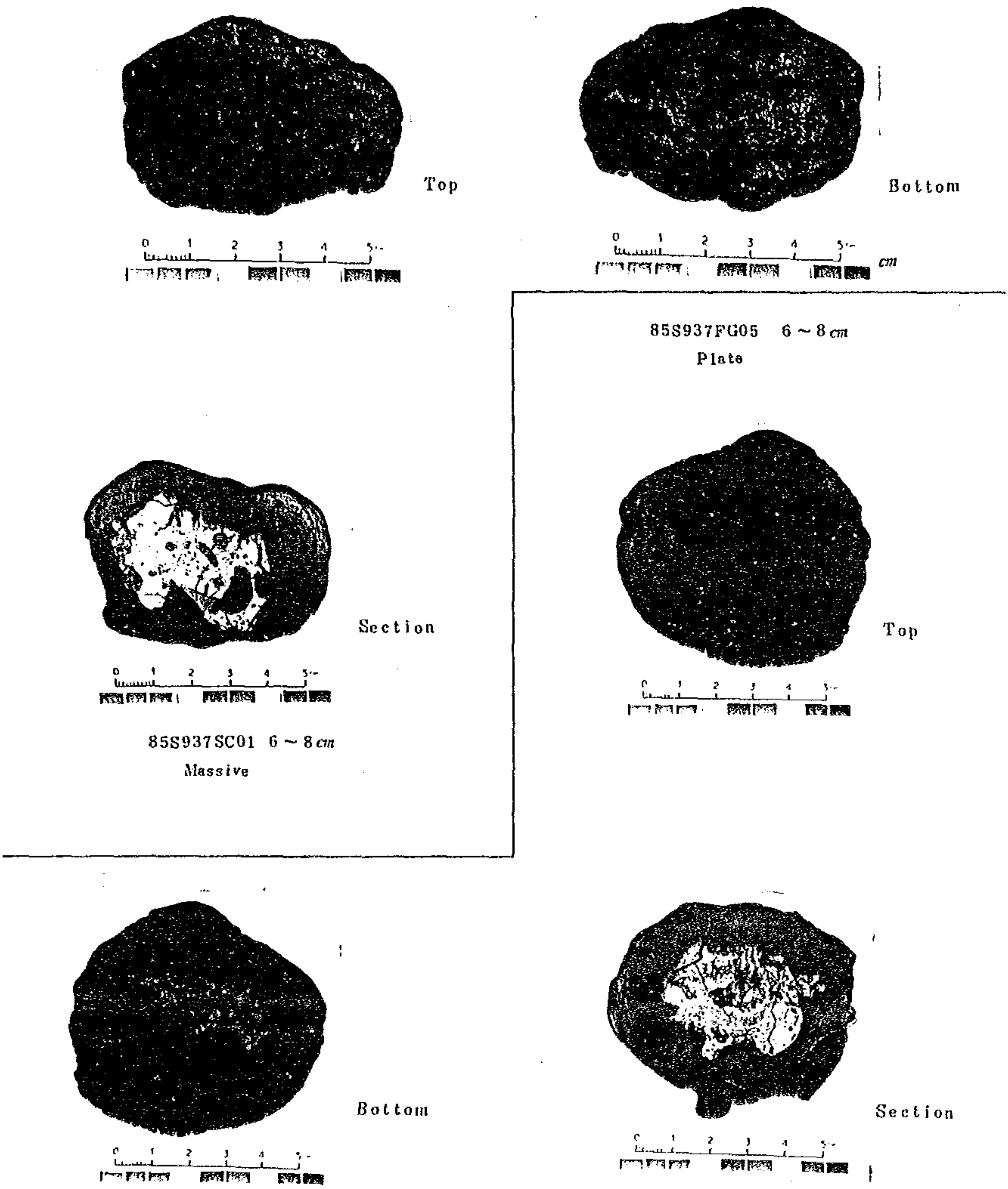

Fig. 4-8-3 Morphology of Manganese Nodules (No.3)

⑥ Plate type (cf. Fig. 4-8-3)

This type has a relatively rough surface with a thin shape like tiles or rice cakes and a round shape varying with small and large size.

⑦ Other type

There are very small nodules whose shape is difficult to be described or stick shaped ones etc.

(2) Size distribution

Fig. 4-8-4 shows the size distribution of manganese nodules. This Fig. indicates clearly that there are mainly small size nodules with 0 - 2 cm and 2 - 4 cm in diameter and that there are very few large nodules.

(3) Characteristics of outward form

The characteristics are shown in the Fig. 4-8-1. The manganese nodules found in the surveyed areas are in general single form type with a relatively rough surface in many cases, except for ellipsoidal type and pebble thin type of nodules. It is remarked that there are few with cracks or fragmentation.

2) Chemical properties
(5 principal components - total analysis - micro-analysis - chemical properties of section)

Fluorescent X-ray analysis for the 5 components (Ni, Cu, Co, Mn and Fe) of each category of size distribution was done on the vessel. Analysis of auxiliary components of representative samples selected from the aforesaid samples was done on shore. Some manganese nodules were divided into several pieces considering their section structure and each of these pieces was analyzed by X-ray. The chemical properties of manganese nodules will be described according to these results. (Statistical consequences should be considered in the light of the small number of samples.)

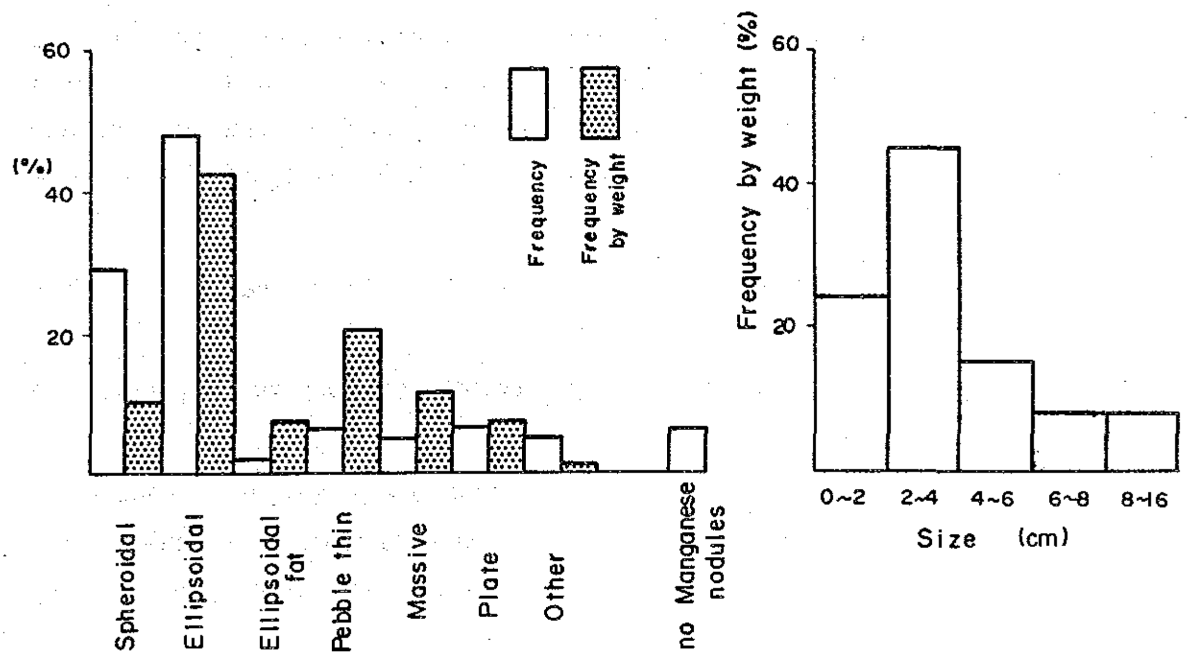

Fig. 4-8-4 Morphology, Size and Sampling Weight of Manganese Nodules

(1) 5 Principal Components

① Grade variation of manganese nodules in the surveyed area

Fig. 4-8-5 shows the frequency distribution of the 5 principal components of manganese nodules in the surveyed areas. Fig. 4-8-6 and Tab. 4-8-2 show respectively a scatter diagram of each components and statistics of the average grade of manganese nodules. Characteristics of the manganese nodules in the surveyed areas are that they have a low Ni, Cu, and Mn content and a high Co and Fe content. Correlation between each component is both positive and negative within that of the Ni-Cu-Mn system and of the Co-Fe system.

② Grade difference according to the morphology of manganese nodules (cf. Tab. 4-8-3)

Characteristics of components according to morphology are as follows:

[1] Spheroidal and ellipsoidal type nodules have a higher Ni and Cu content and a lower Co content than the average grade of manganese nodules in the surveyed areas having about 2 of Mn/Fe ratio.

[2] Ellipsoidal fat type nodules have a low Ni and Cu content and a high Co content contrary to the spheroidal and ellipsoidal type nodules having 1.14 of Mn/Fe ratio. However, the grade of medium size nodules (more than 4 cm in diameter) among the above-mentioned spheroidal type nodules is 0.19% Ni, 0.13% Cu, 0.52% Co, 17.29% Mn and 17.52% Fe (Cu/Ni ratio 0.69, Mn/Fe ratio 0.99) tending to be similar in grade.

[3] Pebble thin and massive type nodules have a low Ni and Cu content and a high Co content having about 1.3 of Mn/Fe ratio.

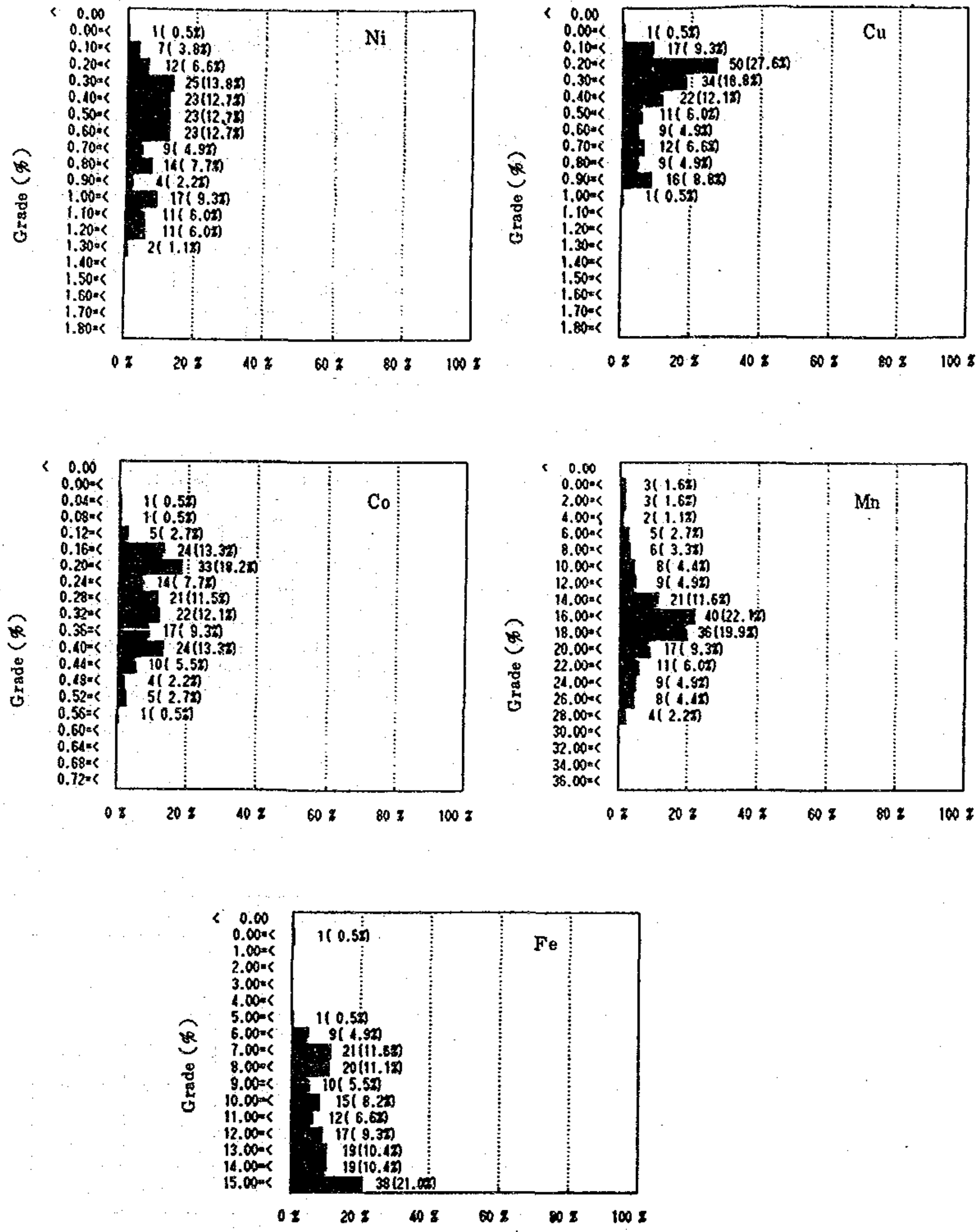

Fig. 4-8-5 Frequency Distribution of 5 Principal Components

Table 4-8-2 Chemical Properties of the Manganese Nodules

(n : 182)

	Statistics (%)				Correlation coeffucient				
	Average	Standard deviation	Maximum	Minimum	Fe	Mn	Co	Cu	Ni
Ni	0.66	0.32	1.34	0.09	−0.76	0.70	−0.60	0.96	1.00
Cu	0.44	0.25	1.00	0.09	−0.77	0.73	−0.62	1.00	
Co	0.30	0.11	0.56	0.05	0.88	0.05	1.00		
Mn	17.35	5.58	28.84	1.35	−0.24	1.00			
Fe	11.79	3.35	18.46	0.84	1.00				

Table 4-8-3 Morphology and Chemical Properties of the Manganese Nodules

Morphology	n	Ni (%)				Cu (%)				Co (%)			
		Average	Standard deviation	Maximum	Minimum	Average	Standard deviation	Maximum	Minimum	Average	Standard deviation	Maximum	Minimum
Spheroidal	40	0.89	1.37	1.34	0.12	0.62	0.27	0.96	0.09	0.27	0.10	0.55	0.17
Ellipsoidal	67	0.72	1.29	1.27	0.24	0.51	0.26	1.00	0.16	0.30	0.10	0.50	0.16
Ellipsoidal fat	4	0.22	0.06	0.26	0.13	0.14	0.02	0.16	0.12	0.53	0.02	0.56	0.52
Pebble thin	23	0.55	1.19	1.07	0.35	0.35	0.13	0.77	0.23	0.39	0.07	0.47	0.21
Massive	17	0.48	0.17	0.87	0.23	0.29	0.10	0.54	0.20	0.30	0.13	0.43	0.05
Plate	27	0.44	0.22	0.87	0.09	0.27	0.11	0.52	0.11	0.28	0.09	0.44	0.14
Other	4	0.54	0.09	0.65	0.44	0.36	0.04	0.40	0.32	0.16	0.03	0.18	0.12

Morphology	n	Mn (%)				Fe (%)				Cu/Ni ratio	Mn/Fe ratio
		Average	Standard deviation	Maximum	Minimum	Average	Standard deviation	Maximum	Minimum		
Spheroidal	40	19.85	4.28	28.52	10.57	10.25	3.27	18.46	6.62	0.68	2.18
Ellipsoidal	67	19.50	4.57	28.84	7.20	11.66	3.32	17.10	6.55	0.68	1.92
Ellipsoidal fat	4	18.30	0.66	19.03	17.43	16.05	0.37	16.54	15.68	0.66	1.14
Pebble thin	23	17.93	2.52	24.41	12.46	13.98	2.19	16.67	7.69	0.63	1.34
Massive	17	13.69	5.60	18.86	1.94	11.20	3.82	15.85	0.84	0.63	1.27
Plate	27	11.47	5.49	20.94	1.35	12.90	2.49	16.10	7.40	0.68	0.92
Other	4	7.58	1.26	8.78	6.17	7.70	1.15	9.21	6.46	0.68	0.99

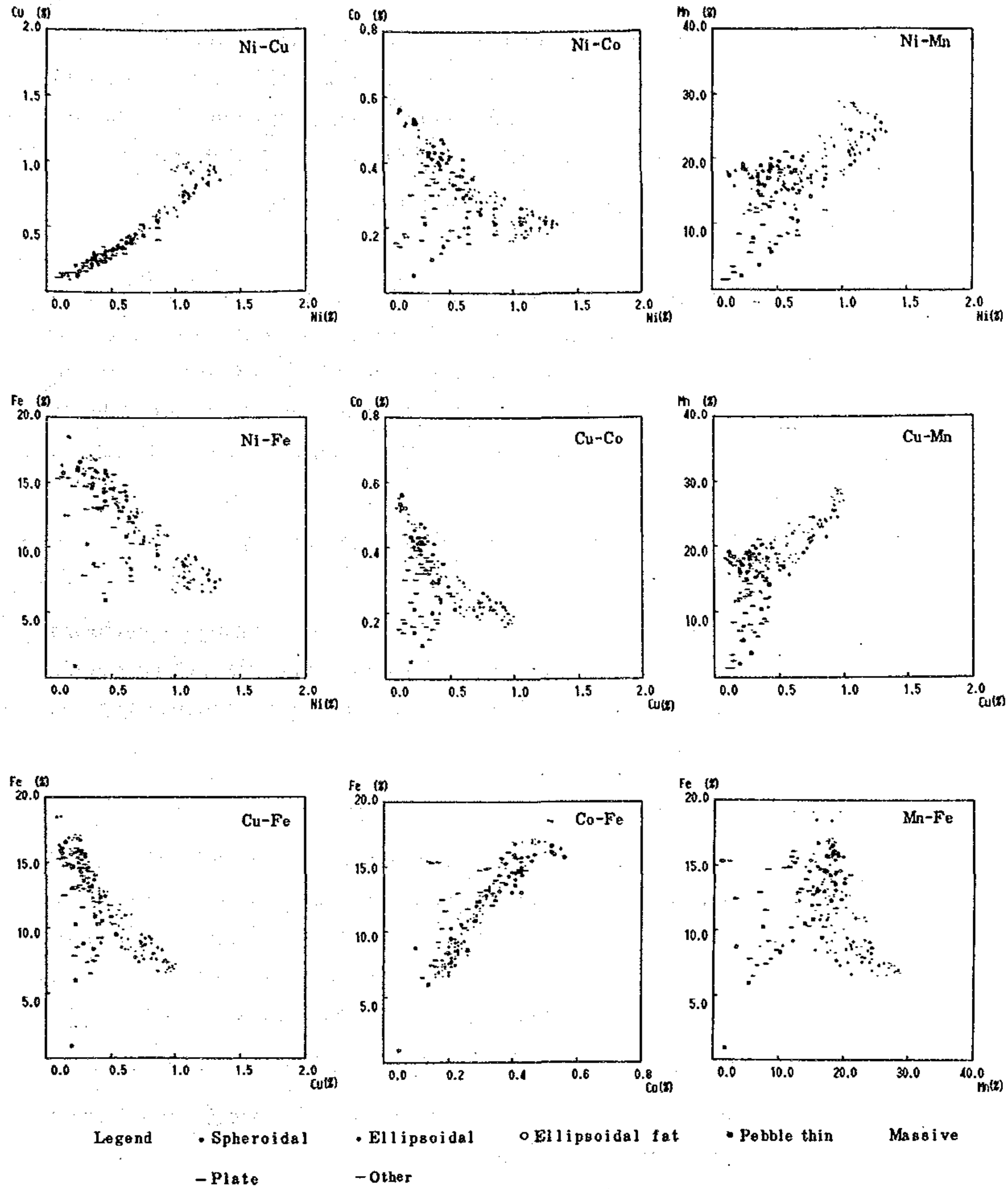

Fig. 4-8-6 Scatter Diagram among Respective Components

[4] Plate and other type nodules have a low Ni and Cu content and a high Co content as well as the pebble thin and massive type nodules having less than 1 of Mn/Fe ratio with slightly higher Fe content than Mn content.

③ Grade difference according to granular size (cf. Tab. 4-8-4)

Smaller manganese nodules (0 - 2 cm and 2 - 4 cm in diameter) having a higher Ni and Cu content and a lower Co content than medium sized nodules (more than 4 cm in diameter). The Mn/Fe ratio of smaller manganese nodules is nearly 2 and that of larger nodules is nearly 1 with a decreasing tendency.

④ Grade difference *1 according to topography (cf. Tab. 4-8-5)

In comparison to the manganese nodules bearing on platforms and sea knolls, nodules bearing on flats have a high Ni and Cu content, while a little bit lower Co content without any great difference.

---

*1 Average grades of manganese nodules described in ①, ②, and ③ show the alithmatic means of assay data for each size group, and those grades in ④ and ⑤ the weighted means of assay data for each sampling stations (number of stations, 114). The average of ④ and ⑤ are as follows:

Ni 0.51%; Cu 0.33%; Co 0.36%; Mn 16.47%; Fe 13.57%.

Therefore, the calculation process of ④ and ⑤ is different from that of ①, ②, and ③.

⑤ Grade difference according to the bottom materials (cf. Tab. 4-8-6)

This grade difference seems to have a similar tendency with the grade difference according to topography as there are overwhelmingly lots of brown clay and calcareous sediment bearing around sea knolls. Namely the manganese nodules bearing among brown clay have a higher Ni and Cu content and a lower Co content than those bearing among calcareous sediment. So the grade difference of cobalt is greater according to the bottom materials than according to the topography.

Table 4-8-4 Size and Chemical Properties of Manganese Nodules

Size (cm)	n	Ni (%)				Cu (%)				Co (%)			
		Average	Standard deviation	Average	Maximum	Average	Standard deviation	Maximum	Minimum	Average	Standard deviation	Maximum	Minimum
0−2	70	0.79	0.34	1.34	0.12	0.53	0.24	0.97	0.14	0.28	0.09	0.46	0.12
2−4	63	0.68	0.27	1.20	0.17	0.47	0.25	1.00	0.12	0.30	0.10	0.51	0.15
4−6	25	0.48	0.27	1.03	0.09	0.33	0.23	0.96	0.11	0.33	0.13	0.55	0.05
6−8	15	0.41	0.18	0.87	0.18	0.24	0.08	0.40	0.09	0.39	0.11	0.52	0.18
8−16	9	0.35	0.17	0.74	0.13	0.24	0.12	0.52	0.12	0.36	0.15	0.56	0.10

Size (cm)	n	Mn (%)				Fe (%)				Cu/Ni ratio	Mn/Fe ratio
		Average	Standard deviation	Maximum	Minimum	Average	Standard deviation	Maximum	Minimum		
0−2	70	17.71	5.43	26.77	1.37	10.97	3.03	17.02	6.46	0.68	1.82
2−4	63	18.34	5.39	28.56	2.51	11.75	3.14	18.46	6.55	0.66	1.77
4−6	25	16.19	6.93	28.84	1.35	12.62	4.25	17.10	0.84	0.70	1.48
6−8	15	15.29	3.89	20.94	8.06	14.47	2.13	18.42	10.18	0.59	1.06
8−16	9	14.34	4.92	19.03	3.56	13.10	3.16	16.07	8.47	0.69	1.09

Table 4-8-5 Sea Floor Topography and Cheical Properties of Manganese Nodules

Topography	n	Ni (%)				Cu (%)				Co (%)			
		Average	Standard deviation	Maximum	Minimum	Average	Standard deviation	Maximum	Minimum	Average	Standard deviation	Maximum	Minimum
Flat	65	0.55	0.29	1.34	0.13	0.36	0.22	0.98	0.12	0.36	0.12	0.55	0.10
Hollow	1	0.16	–	–	–	0.15	–	–	–	0.16	–	–	–
Platform	7	0.46	0.11	0.87	0.38	0.28	0.06	0.56	0.22	0.38	0.05	0.44	0.17
Knoll	9	0.46	0.15	0.93	0.25	0.29	0.09	0.59	0.17	0.37	0.09	0.47	0.21
Rest	3	0.46	0.17	0.60	0.18	0.28	0.11	0.36	0.09	0.41	0.06	0.52	0.38

Topography	n	Mn (%)				Fe (%)			
		Average	Standard deviation	Maximum	Minimum	Average	Standard deviation	Maximum	Minimum
Flat	65	17.25	4.54	28.61	3.56	13.00	3.34	16.91	4.99
Hollow	1	2.23	–	–	–	15.30	–	–	–
Platform	7	16.16	1.52	21.38	7.20	14.79	1.60	16.21	8.75
Knoll	9	15.17	3.82	18.34	5.52	13.90	1.96	15.86	8.96
Rest	3	19.00	0.51	10.20	18.02	15.28	2.09	18.42	13.30

Table 4-8-6 Bottom Sediments and Chemical Properties of Manganese Nodules

Sediment	n	Ni (%)				Cu (%)				Co (%)			
		Average	Standard deviation	Maximum	Minimum	Average	Standard deviation	Maximum	Minimum	Average	Standard deviation	Maximum	Minimum
Brown clay	79	0.52	0.27	1.34	0.13	0.34	0.20	0.98	0.12	0.35	0.12	0.55	0.10
Zeolotic clay	1	0.68	–	–	–	0.37	–	–	–	0.30	–	–	–
Calcareous sediment	3	0.42	0.03	0.45	0.37	0.27	0.01	0.28	0.24	0.42	0.05	0.47	0.30

Sediment	n	Mn (%)				Fe (%)			
		Average	Standard deviation	Maximum	Minimum	Average	Standard deviation	Maximum	Minimum
Brown clay	79	16.42	5.06	28.61	2.23	13.25	3.03	16.91	4.99
Zeolotic clay	1	14.98	–	–	–	11.43	–	–	–
Calcareous sediment	3	16.71	1.40	18.34	14.45	15.93	0.65	16.21	13.04

(2) Auxiliary components

Total analysis and small quantity analysis were done ashore on 3 samples selected from samples used for the 5 principal components analysis on the vessel in order to investigate the auxiliary component properties of manganese nodules. Tab. 4-8-7 shows both the total and small quantity analysis values and that of the 5 principal components analysis on the vessel. The SiO_2, TiO_2, Al_2O_3, CaO, K_2O, P_2O_5, Pb, Sr, V, B and Y components of manganese nodules in the surveyed areas have a higher grade than the average grade *1 in the Clarion-Clipperton Prime area by Mckelvey et al (1979). The reason for the higher grade of SiO_2 and Al_2O_3 seems to be the influence of external origin materials (such as rock pieces). On the contrary, MgO, BaO, Na_2O, Mo and Zn have a lower grade than the average grade in the Clarion-Clipperton Prime area.

(3) Chemical properties of sections of manganese nodules

Manganese nodules have growing structures of concentricly circled layers of manganese minerals with a core of a fragment of ancient manganese nodules or a core of external origin materials (such as rocks, teeth of sharks, authigenic minerals, clay).

Manganese nodules in the surveyed areas rarely have a core of a fragment of ancient manganese nodules and have mainly a core of external origin materials. A small amount of nodules have their sections with a clear concentricly circled structure when observed with the naked eye. This also seems to be a part of the

---

*1 Si 7.81%, Ti 0.61%, Al 2.84%, Mg 1.80%, Ca 1.47%, Ba 0.32%, Na 1.87%, K 0.82%, P 0.23%, Pb 0.048%, Sr 0.066%, Mo 0.048%, V 0.03%, B 0.016%, Zn 0.13%, Y 0.01%

Table 4-8-7 Chemical Composition of Manganese Nodules

	Sampling No.	85S736FG02	85S936FG02	85S936FG05
Topography		(Hilly) Flat	(Hilly) Flat	(Hilly) Platform
Depth (m)		4,944	5,510	5,152
Morphology		Plate	Spheroidal and Ellipsoidal fat	Ellipsoidal
Size (cm)		8−16	4−6	4−6
X.R.F. analyses (%)	Ni	0.39	0.12	0.40
	Cu	0.24	0.11	0.26
	Co	0.26	0.55	0.39
	Mn	9.75	17.78	15.66
	Fe	8.47	16.31	15.27
Major element (%)	SiO_2	38.18	15.77	23.35
	TiO_2	0.92	1.72	1.77
	Al_2O_3	10.25	5.28	5.46
	Fe_2O_3	11.50	24.12	21.70
	FeO	<0.01	<0.01	<0.01
	MnO_2	16.06	29.04	25.07
	MgO	2.52	1.93	2.17
	CaO	2.18	2.38	2.16
	BaO	0.06	0.07	0.10
	Na_2O	2.45	2.14	1.95
	K_2O	2.22	0.63	0.87
	P_2O_5	1.00	0.74	0.69
	Ig−loss	11.90	15.67	14.21
Minor element (%)	Pb	0.039	0.095	0.075
	Sr	0.051	0.095	0.080
	Mo	0.017	0.037	0.034
	V	0.027	0.091	0.068
	As	0.006	0.014	0.012
	B	0.043	0.074	0.069
	Zn	0.038	0.042	0.051
	Y	0.018	0.008	0.014

reason for their low Ni and Cu content. In order to examine the chemical properties of sections, 2 circular boundary seams (inside and outside) were set up on the sections, as a matter of convenience, and these boundary seams divided the sections into 3 parts; the core encircled by a inside boundary, the inner crust enclosed by two boundaries and the outer crust formed by the external part of a outside boundary. Further to this rough division, each of these parts were divided into several smaller parts. Fluorescent X-ray analysis were carried out on these small parts researching for the 5 principal components.

Tab. 4-8-8 shows the analysis results of manganese nodules; Fig. 4-8-7 and 4-8-8 show respectively the dividing positions of each sample and the grade of each section according to respective nodules shapes. General comments are as follows:

① The top surface of the outer crust may have a lower Ni and Cu content and a higher Co content than the bottom surface of the outer crust.

② Except for the spheroidal type, the outer crust may have a trend of presenting a higher grade of Ni and Cu than the inner crust.

③ The core has a lower Ni, Cu and Co content than the outer and inner crusts; that indicates the core would be composed of external origin materials. On the other hand, the core of the pebble thin type nodules has a higher Ni content than the outer and inner crusts.

3) Mineral properties (X-ray diffraction analysis - microscopic observation)

Concerning the representative samples, X-ray diffraction analysis and observation of polished thin sections by microscope were done in order to investigate the mineral composition and inner structure of manganese nodules.

Table 4-8-8 Chemical Compositional Difference Between Surface and Inner Part Nodules

Sample No.	Size (cm)	Morphology	Analyse position		XRF Analyses (%)					Cu/Ni	Mn/Fe
					Ni	Cu	Co	Mn	Fe		
85S 836FG07	6−8	Spheroidal	Upper	Outer crust	0.19	0.09	0.51	17.57	19.13	0.47	0.92
				Inner crust 1	0.30	0.16	0.46	18.56	16.80	0.53	1.10
				Inner crust 2	0.34	0.17	0.42	17.91	14.60	0.50	1.23
				Core	0.28	0.15	0.37	14.44	14.70	0.54	0.98
			Lower	Core	0.05	0.16	0.03	0.05	7.00	3.20	7.14
				Inner crust 2	0.23	0.12	0.48	17.98	16.81	0.52	1.07
				Inner crust 1	0.26	0.14	0.50	18.81	17.30	0.54	1.09
				Outer crust	0.21	0.10	0.58	15.64	18.78	0.48	0.83
85S 836FG05	8−16	Ellipsoidal	Upper	Outer crust	0.29	0.18	0.54	19.54	17.59	0.62	1.11
				Inner crust 1	0.18	0.10	0.56	20.58	17.32	0.56	1.19
				Inner crust 2	0.24	0.09	0.58	19.25	15.00	0.38	1.28
			Core		0.06	0.05	0.19	4.04	12.18	0.83	0.33
			Lower	Inner crust 2	0.22	0.11	0.53	19.40	16.09	0.50	1.21
				Inner crust 1	0.25	0.13	0.55	20.00	17.30	0.52	1.16
				Outer crust	0.52	0.31	0.49	20.52	16.34	0.60	1.26
85S 936FG05	4−6	Pebble thin	Upper	Outer crust	0.19	0.09	0.46	14.71	21.25	0.47	0.69
			Core		0.46	0.19	0.19	7.89	9.04	0.41	0.87
			Lower	Inner crust 2	0.29	0.21	0.40	16.61	16.23	0.72	1.03
				Inner crust 1	0.39	0.33	0.43	18.32	17.11	0.85	1.07
				Outer crust	0.43	0.36	0.42	19.17	17.12	0.84	1.12
85S 937FG03	6−8	Massive	Upper	Outer crust	0.43	0.27	0.47	20.58	14.98	0.63	1.37
				Inner crust 1	0.33	0.18	0.45	18.34	13.25	0.55	1.38
			Inner crust 2		0.39	0.21	0.44	18.02	12.61	0.54	1.43
			Core		0.21	0.13	0.26	9.15	11.98	0.62	0.76
			Lower	Inner crust 1	0.32	0.18	0.38	17.73	12.62	0.56	1.40
				Outer crust	0.43	0.28	0.46	19.46	14.58	0.65	1.33

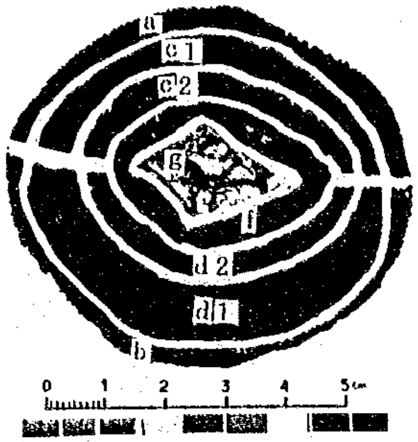

85S836FG07 (6 ~ 8 cm)
Spheroidal

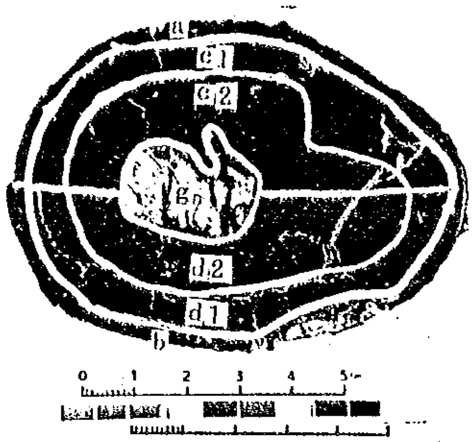

85S836FG05 (8 ~ 15 cm)
Ellipsoidal fat

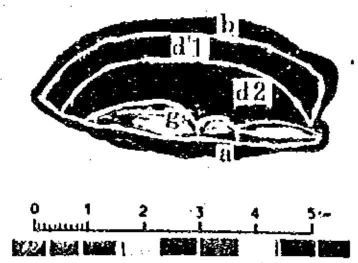

85S936FG05 (4 ~ 6 cm)
Pebble thin

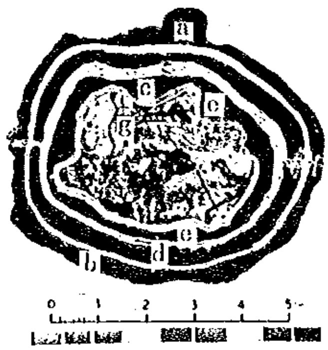

85S937FG03 (6 ~ 8 cm)
Massive

Legend

a : Outer Crust Upper　　b : Outer Crust Lower part
c : Inner Crust Upper part　　d : Inner Crust Lower part
e : Inner Crust 2　　f : Inner Crust 3　　g : Core

Fig. 4-8-7 Photos of Manganese Nodules used for Section Analysis

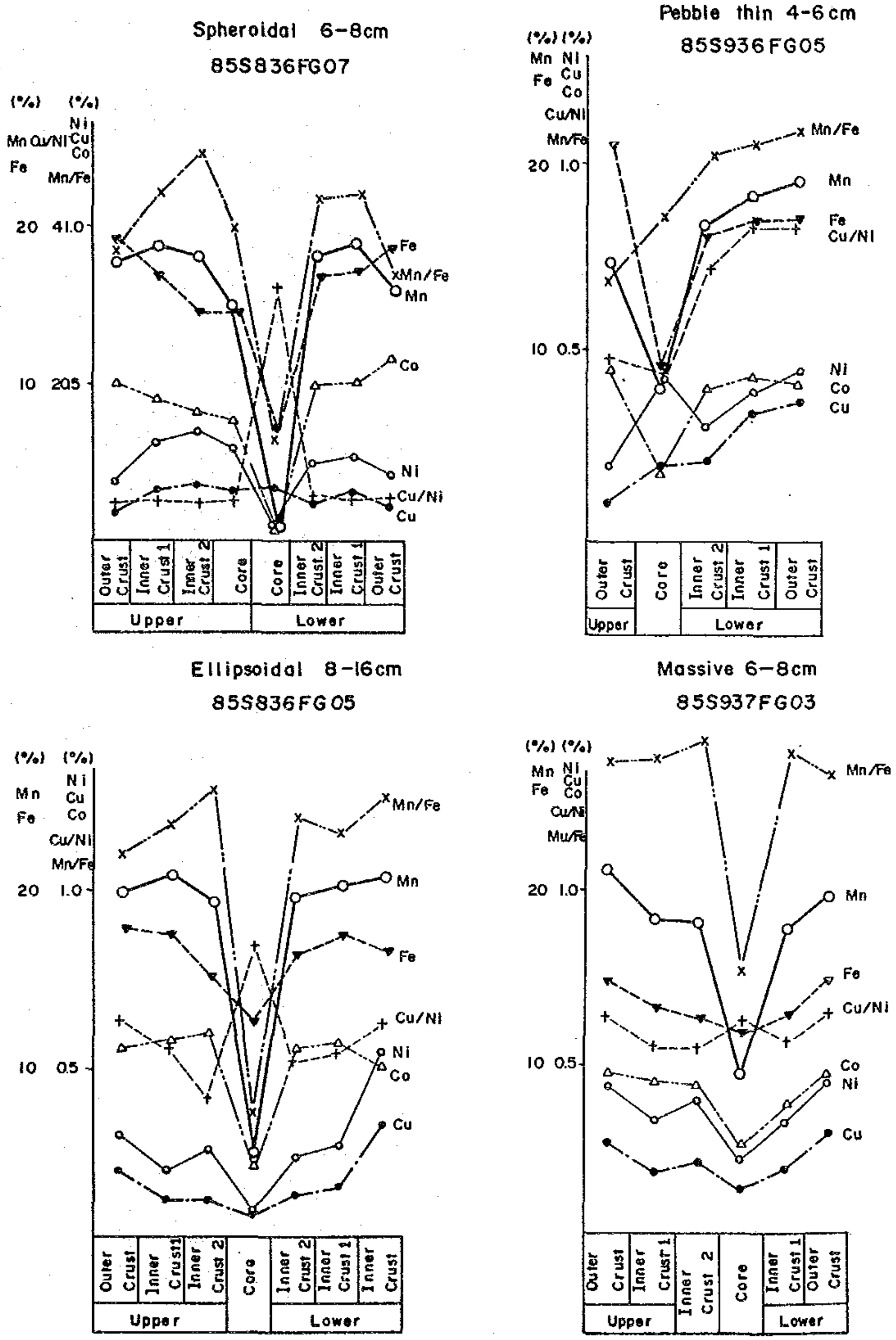

Fig. 4-8-8 Grade of Respective Section of Manganese Nodules

(1) X-ray diffraction analysis

Manganese nodules were roughly divided into the outer crust, inner crust and core; moreover, each of the samples shown in Fig. 4-8-9 was divided into several smaller parts on which X-ray diffraction analysis was executed. The results of analysis are indicated in Tab. 4-8-9 and the X-ray diffraction patterns are in Fig. 4-8-10.

Detected minerals are quartz, plagioclase, montmorillonite, illite, phillipsite and 3 kinds of manganese minerals: 10Å manganite, δ-MnO_2 and 7Å manganite with a low peak of X-ray diffraction. Particularly, manganese minerals were not observed in the core and a high peak of the diffraction chart related to other minerals than manganese (such as wellsite) appeared; these are presumably external origin materials.

(2) Observation by microscope

Polished thin sections were prepared from the representative samples of manganese nodules and observation was done by microscope with transmitted and reflected light. Explanations will be made on a typical sample of the manganese nodules of ellipsoidal fat type.

Characteristics of the ellipsoidal fat type (85S-936FG02 8 - 16 cm) are as follows:

Observation with naked eye:

External appearance: an oval and bulgy shape, like that of two integrally combined spheres and seemed to be a variation of the medium or large sized spheroidal type of manganese nodule.

The aspect of surface both at the top and the bottom is coarse and this type of manganese nodules occurs characteristically in the surveyed areas.

As shown by the macro-photo of section in Fig. 4-8-11 the core is composed of external origin materials and occupies a greater

Table 4-8-9 Results of X-ray Diffraction Analysis of the Manganese Nodules

Sample No.	Size (cm)	Morphology	Analyse position		10Å	7Å	δ-Mn	Q	Pℓ	Mo	Ph	I
85S936FG01	8−16	Ellip-soidal	Outer crust	Upper	+		±	+	+			
				Lower	+		±	+	+		+	
			Inner crust	Upper	+			+	+		++	
				Lower	+			+	+		+	
			Core					+	++			
85S936FG02	4−6	Ellip-soidal fat	Outer crust	Upper	+		±	+	+		±	
				Lower	+	±		+	+			
			Inner crust	1 Upper	+		±	+	+		+	
				1 Lower	+	±	±	+	+		+	
				2	+		±	++	+		+	
			Core					+	++	+	+++	
85S837FG06	6−8	Plate	Outer crust	Upper	+		±	+	+			
				Lower	+		±	+	+		+++	
			Inner crust upper		±			+	+		++	
			核					+	+		+++	±

Legend

10Å: 10Å manganite　　7Å: 7Å manganite　　δ-Mn: δ-MnO_2　　Q: Quartz

Pl: Plagioclase　　Mo: Montmorillonite　　Ph: Phillipsite　　I: Illite

+++: very strong　　++: strong　　+: weak　　±: very weak

Intensity of diffraction line

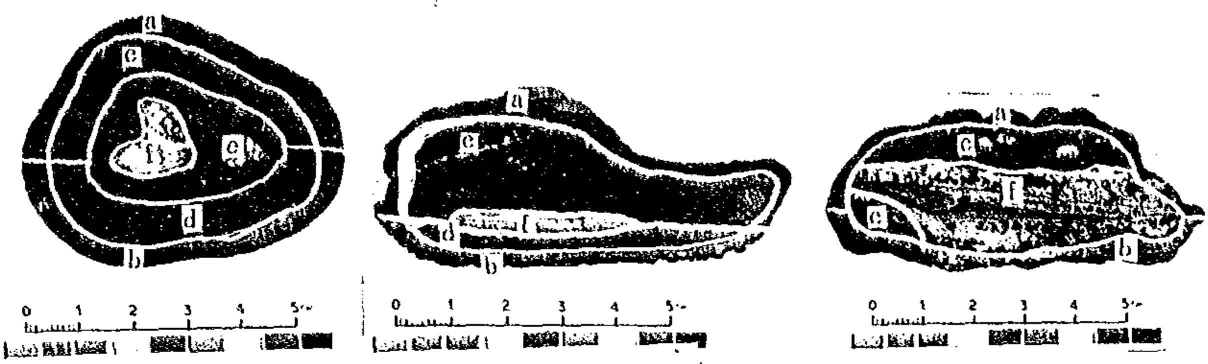

85S936FG2 (4 ~ 6 cm)
Ellipsoidal fat

85S936FG01 (8 ~ 16 cm)
Ellipsoidal

85S837FG06 (6 ~ 8 cm)
Plate

Legend

a : Outer Crust Upper part
b : Outer Crust Lower part
c : Inner Crust Upper part
d : Inner Crust Lower part
e : Inner Crust 2
f : Core

Fig. 4-8-9 Photos of Manganese Nodules used for X-ray Diffraction Analysis

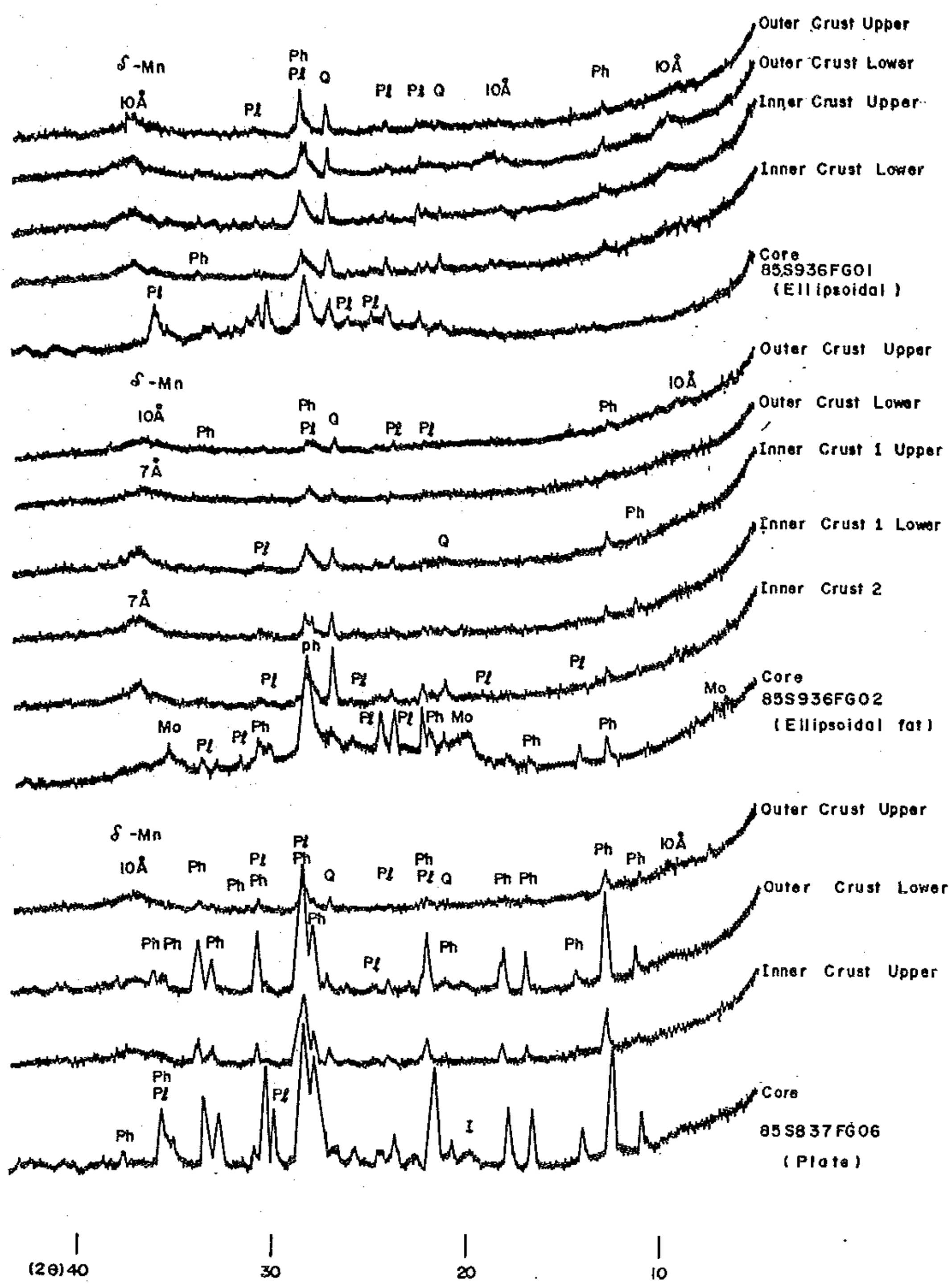

Legend
10Å : 10Å manganite 7Å : 7Å manganite δ-Mn : δ-MnO_2 Q : Quartz
Pl : Plagioclase Mo : Montmorillonite I : Illite Ph : Phillipsite

Fig. 4-8-10 X-ray Diffraction Patter of Manganese Nodules

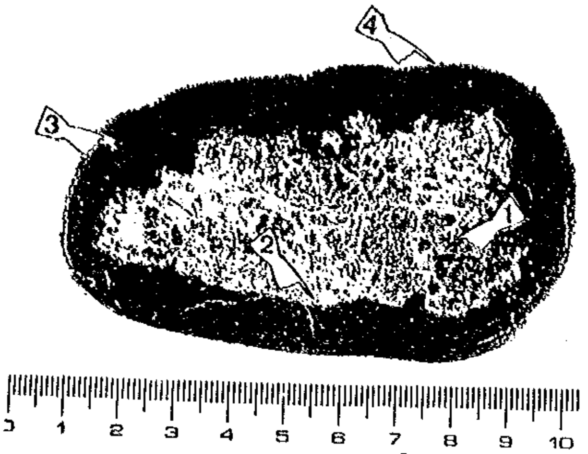

I Section
transmitted light

(85S936FG02)
Ellipsoidal fat
I. Section
number of this photo shows
micro-photo's position
II–1~4 Micro photo
Legend
T: 10Å Manganite
D: δ-MnO_2
Clay: Clay minerals
scale bar: 0.5㎜

II – 1 (Core)

II – 2 (Core and Outer Crust)

reflected light
transmitted light

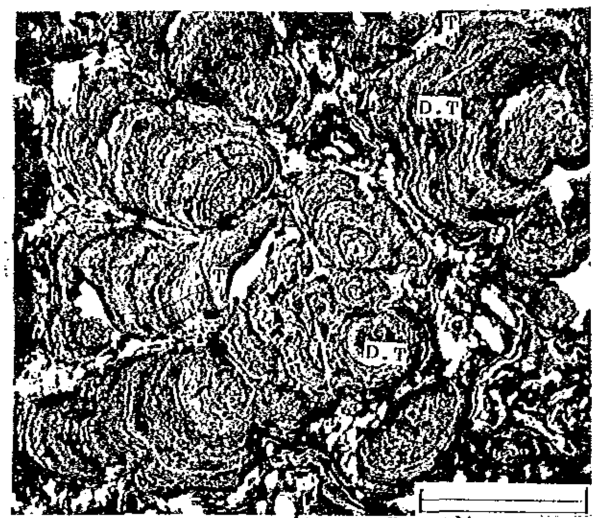

II – 3 (Outer Crust)

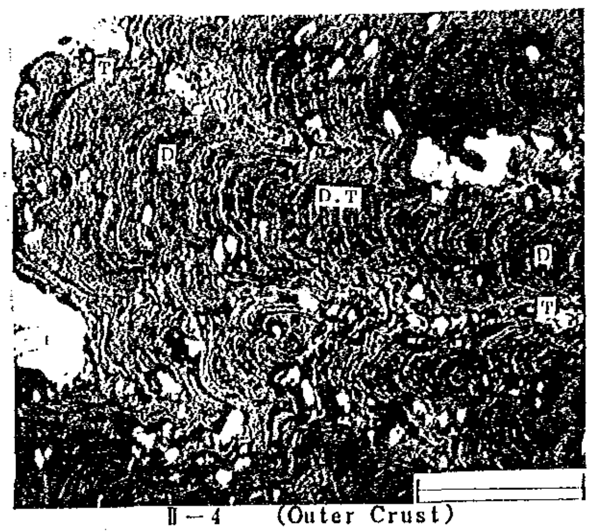

II – 4 (Outer Crust)

reflected light
transmitted light

Fig. 4-8-11 Macro-photo and Microscopic Photos of Polished Thin Section of Manganese Nodules

part of the manganese nodule. The principal manganese minerals are found at the outer crust with a width of 1.0 - 1.5 cm and the concentricly circled structure is not so clear.

Observation by microscope:

The core is composed of a great volume of clay minerals and contains pieces of manganese minerals (cf. Photo No. I of Fig. 4-8-11); it is remarked that the part of core in contact with the outer crust embraces pieces of manganese minerals (cf. Photo No. II-2 left side of Fig. 4-8-11)

The outer crust has a regular striped texture of manganese minerals (10Å manganite and δ-MnO_2), a grape-like texture (cf. Photos No. II-2 right side and No. II-4 of Fig. 4-8-12) and a variole-like texture (cf. Photo No. II-3 of Fig. 4-8-12)

4) Distributional characteristics of manganese nodules

(1) Morphology distribution of manganese nodules

As for the morphology distribution of manganese nodules, the following rough classification was set up:

- zone where ellipsoidal type is superior
- zone where massive and pebble thin type are superior
- medium morphology zone.

These zones are marked on the morphology map as shown in the Fig. 4-8-12.

In the surveyed areas, a lot of medium morphology zones are found and in the areas surrounding sea knolls, massive and pebble thin type zone are more common.

(2) Size distribution of manganese nodules

Fig. 4-8-13 shows the average size distribution of manganese nodules. Small sized manganese nodules (0 - 2, 2 - 4 cm) are the majority from the center to eastern part in the surveyed areas. Middle size (more than 4 cm) are distributed in the surroundings of sea knolls in the western part of the areas.

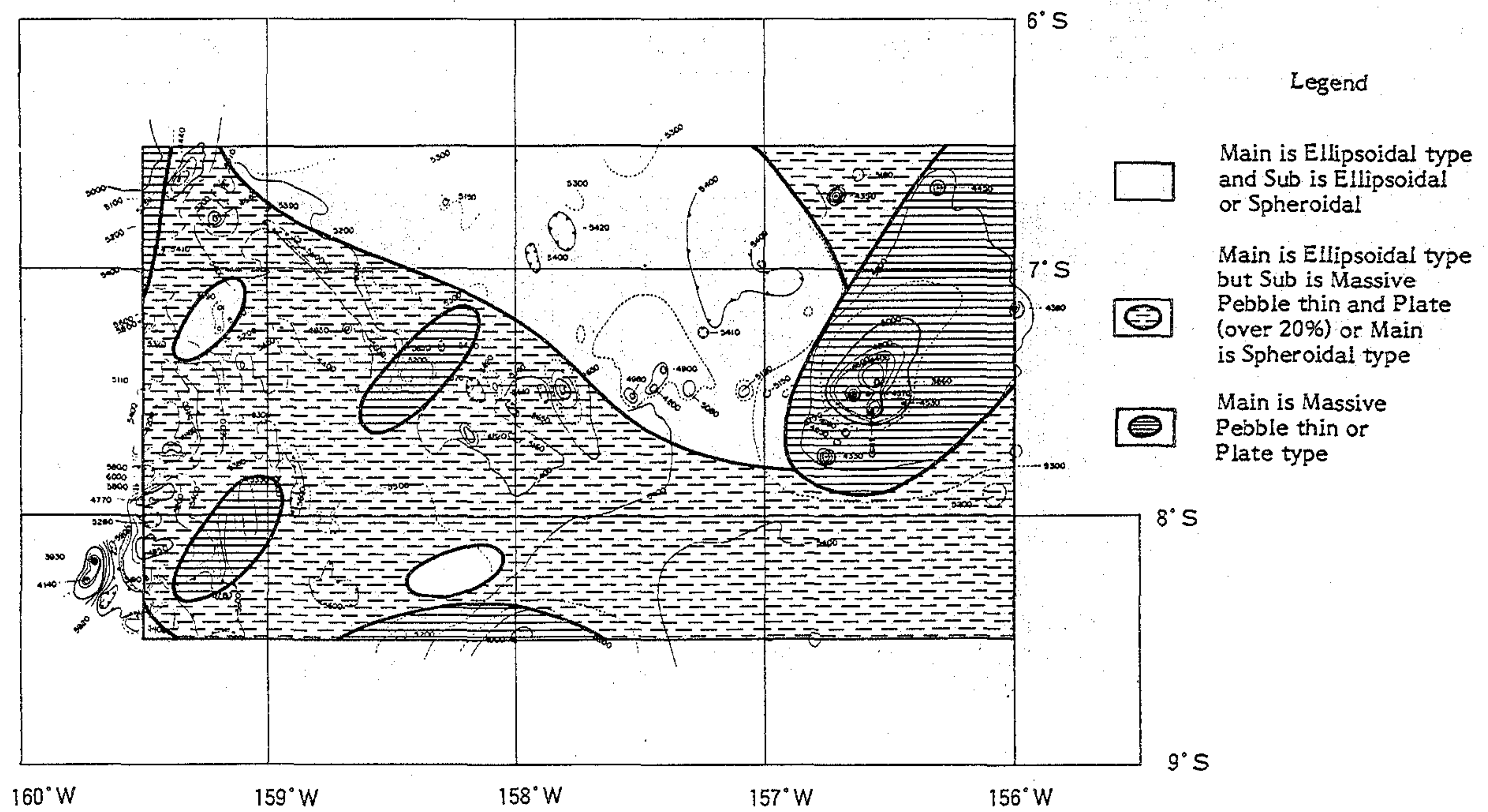

Fig. 4-8-12 Morphology Distribution of Manganese Nodules

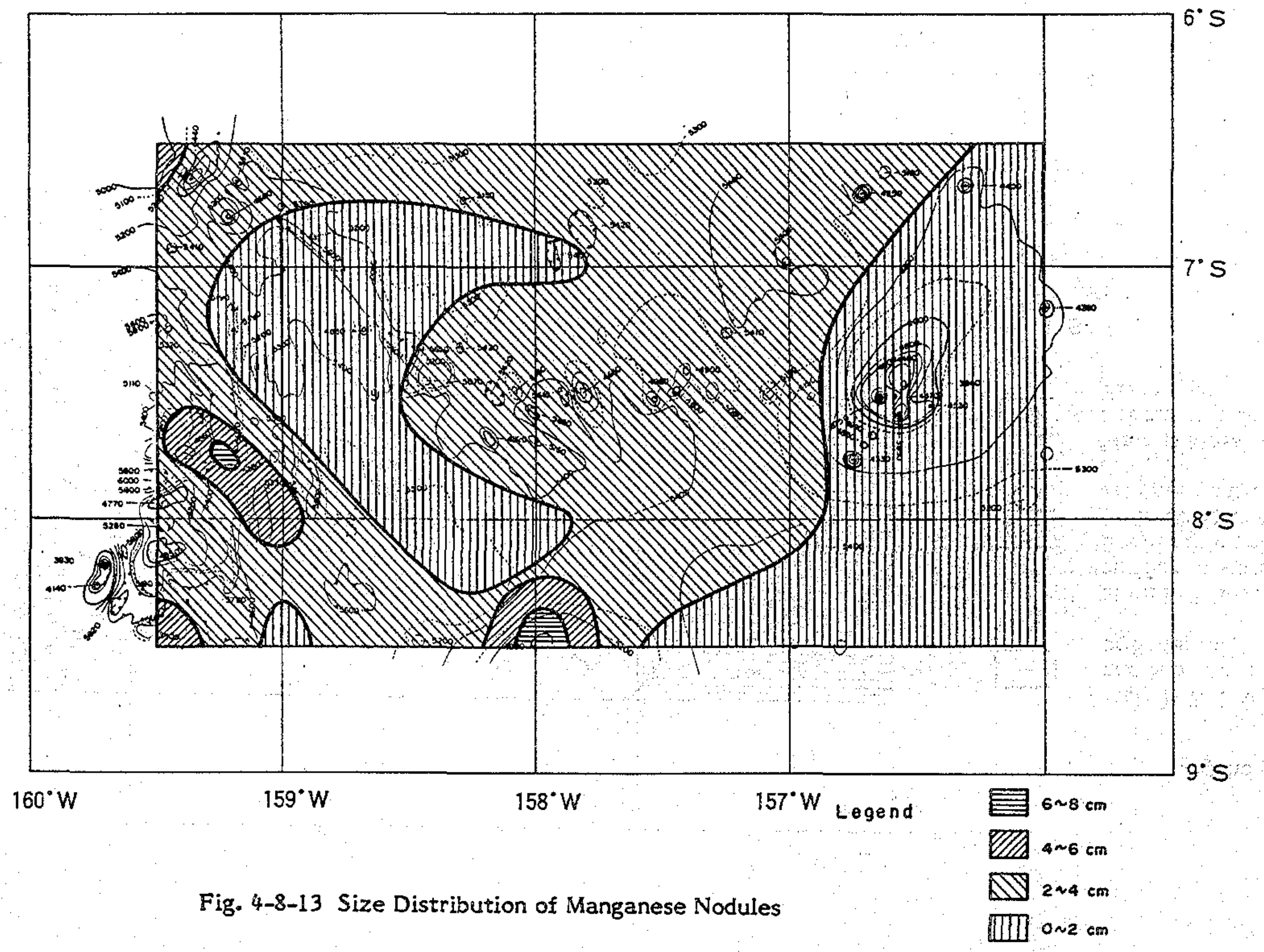

Fig. 4-8-13 Size Distribution of Manganese Nodules

(3) Granular size and morphology

The morphological classification ratio of the manganese nodules by respective granular size are shown in Fig. 4-8-14.

Except 8 - 16 cm size, ellipsoidal fat type are the majority of the manganese nodules, secondly, spheroidal type 0 - 2 cm size, pebble thin type for 2 - 4 and 4 - 6 cm size and massive type for 6 - 8 cm.

The percentage of pebble thin and massive types increase gradually for 2 - 4, 4 - 6 and 6 - 8 cm size compared with 0 - 2 cm size. For 8 - 16 cm size, ellipsoidal fat type is the majority, with being second in quantity, ellipsoidal type.

(4) Local-topography and morphology

The morphological classification ratio of manganese nodules by respective Local-topography is shown in Fig. 4-8-15. The percentage of pebble thin and massive type has a trend of getting greater except in the flat. As for the metal content, Ni and Cu content are low and Co is high in pebble thin and massive types. These phenomena are concordant with the fact that they have the same tendency in Local-topography.

(5) SBP type and morphology

The morphological classification ratio by respective SBP type and thickness of upper transparent layers (*1) are shown respectively in Fig. 4-8-16 and 4-8-17. Pebble thin and massive type nodules are present in type b with upper transparent layers; in types c, ds and d2 without them.

They are not present in type a and e1 with upper transparent layers.

---

*1 Collecting the statistics based on datas for 10 m unit of upper transparent layers.

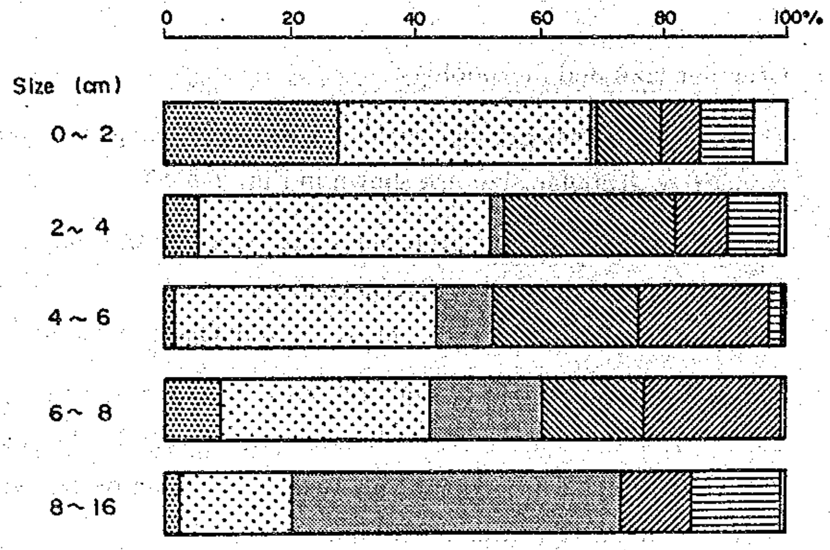

Fig. 4-8-14 Relation between Size and Morphology

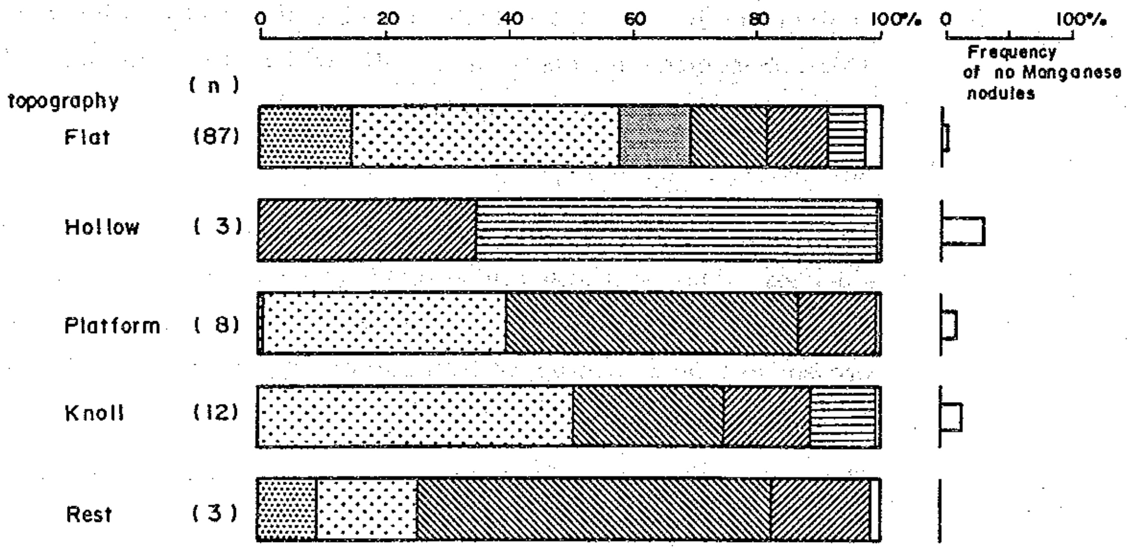

Fig. 4-8-15 Relation between Local Topography and Morphology

Legend

Spheroidal, Ellipsoidal, Ellipsoidal fat, Pebble thin, Massive, Plate, Other

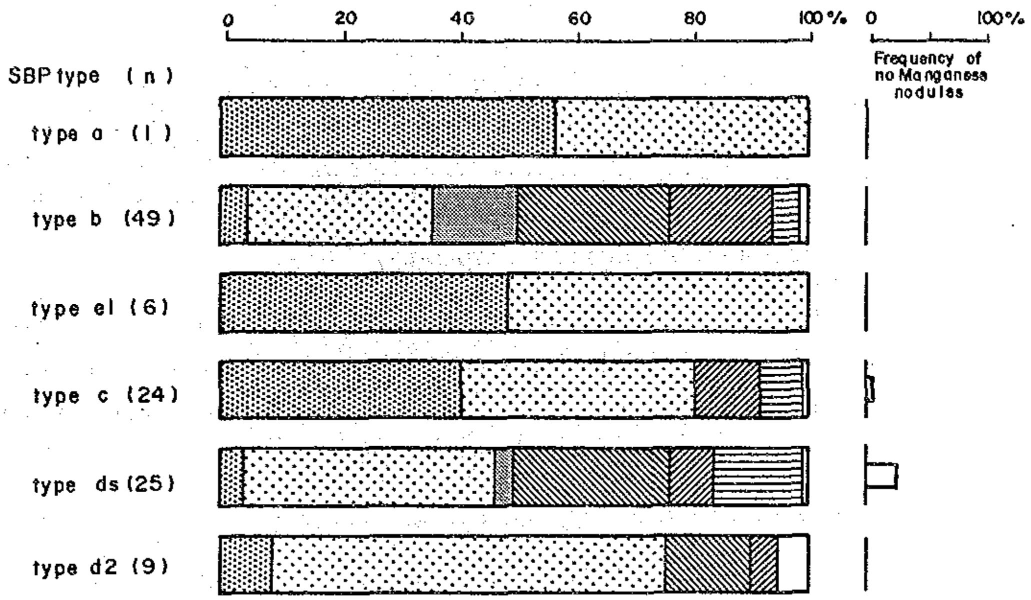

Fig. 4-8-16 Relation between SBP Type and Morphology

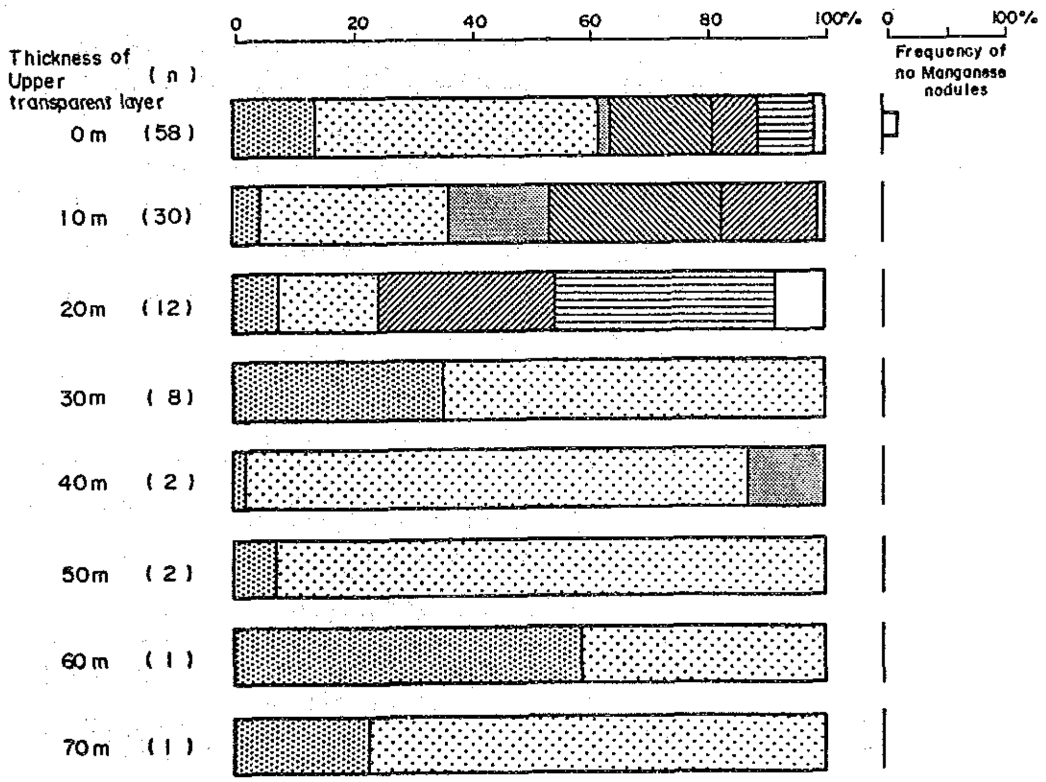

Fig. 4-8-17 Relation between Upper Transparent Layer Thickness and Morphology

When the thickness of upper transparent layers is 0, 10 and 20 m, pebble thin and massive types appear, therefore, these appeared even in type b with relatively thin upper transparent layers.

(6) Bottom materials and morphology

Fig. 4-8-18 shows morphological classification ratio by respective bottom materials. It has a tendency to make the ratio of pebble thin type higher in calcareous sediment that is distributed near sea knolls, compared with brown clays.

5) Sea bottom situation and abundance

(1) Morphology and abundance of manganese nodules

Fig. 4-8-19 shows the average abundance and occurrence ratio of abundance by respective morphology.

Morphology of high average abundance is mostly pebble thin type except for two sampling points with a ellipsoidal fat. The morphology of 0 abundance is not pebble thin type.

The morphology of massive and plate types indicate higher abundance than that of the ellipsoidal fat type. But it is caused by the inclusion of a lot of massive type in medium and large size manganese nodules.

(2) Sea floor topography and abundance

At each sampling points, the relation between the sea bottom and the abundance of manganese nodules is shown in Table 4-8-10.

Table 4-8-10 Relation Between Regional Sea Floor Topography and Abundance of Manganese Nodules

Topography	No. of sampling points	Average abundance	Occurrence ratio $\geqq 5$ kg/m^2
Plain	81	1.61 kg/m^2	6%
Hilly	33	7.04	64

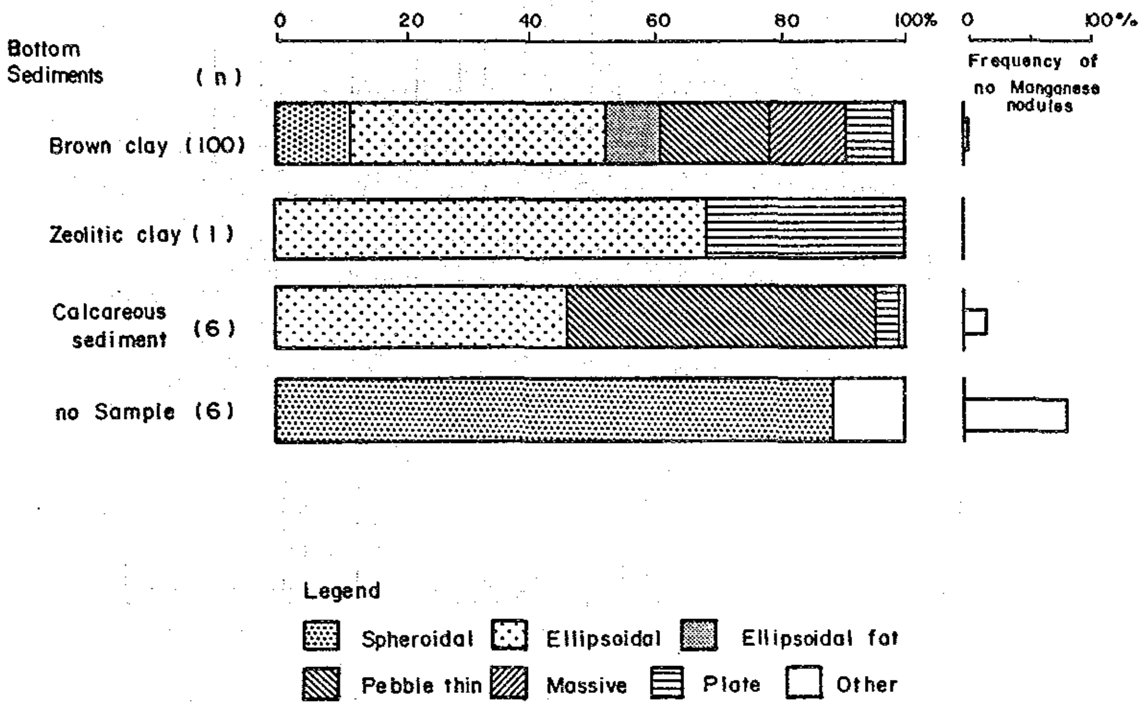

Fig. 4-8-18 Relation Between Bottom Sediments and Morphology

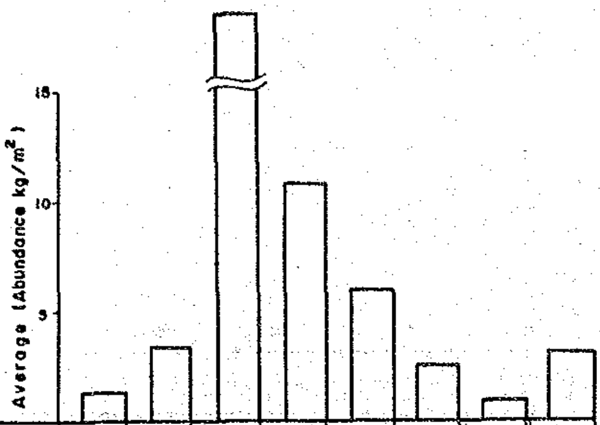

Morphology	Sphe-roidal	Ellip-soidal	Ellipso-idal fat	Pebble thin	Massive	Plate	Other	Total
Arerage (Abundance kg/m²)	1.11	3.10	18.52	10.78	5.99	3.55	0.90	3.19
Standard deviation	1.15	4.95	18.89	3.00	4.92	3.71	1.17	5.15
Number of saples	30	51	2	7	5	7	5	114

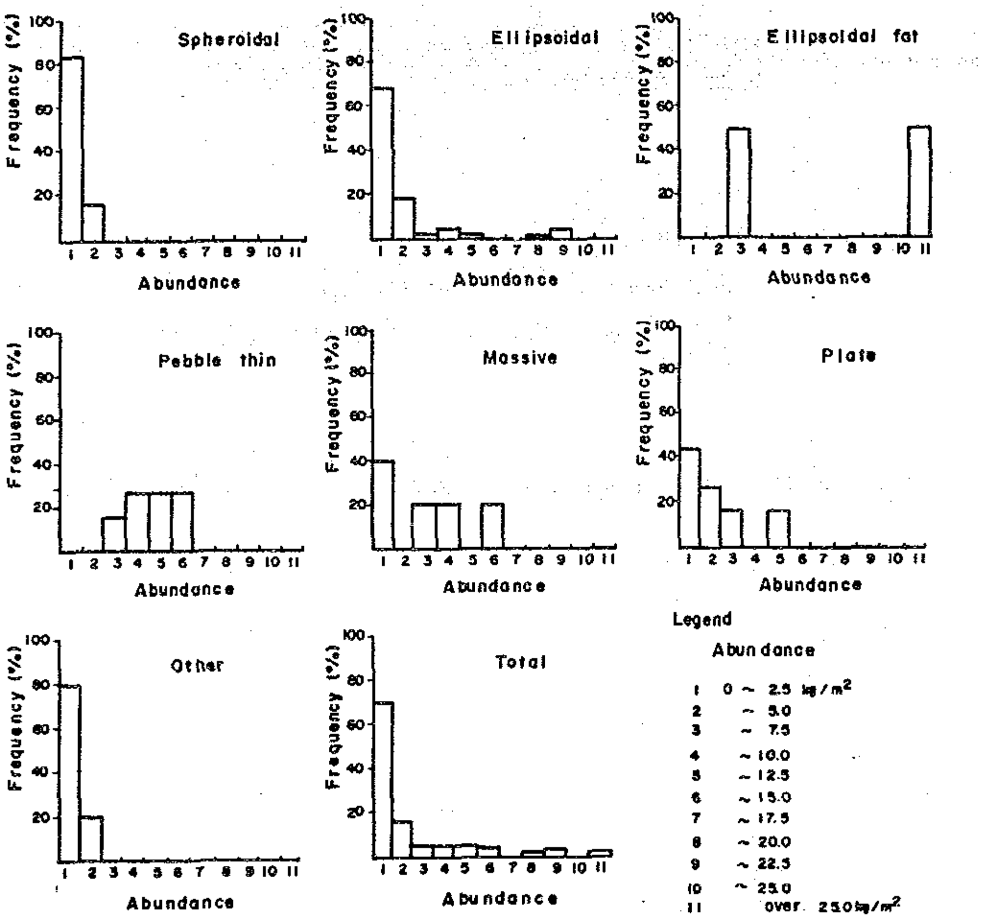

Fig. 4-8-19 Average Abundance by Respective Morphology and Occurrence Ratio by Respective Abundance of Manganese Nodules

The present areas are divided, from macroscopic point of view, by the longitudinal line 159°W into the plain of the eastern part and the hill of the western part. As being evident from Table 4-8-10, the abundance of manganese nodules for plains is low (average 1.61 kg/m^2) and the occurrence ratio of more than 5 kg/m^2 is only 6%. On the other side, the hills indicate high average abundance (7.04 kg/m^2) and occurrence ratio of 64% (more than 5 kg/m^2). In the surveyed areas, the area with an abundance of more than 5 kg/m^2 are found almost all on the hills. The statistical results of plains and hills observed microscopically are shown in Table 4-8-11 and 4-8-12.

Table 4-8-11 Relation Between Local Sea Floor Topography and and Abundance of Manganese Nodules in Plain Province

Topography	No. of sampling points	Average abundance	Occurrence ratio $\geqq 5\ kg/m^2$
Flat	72	1.32 kg/m^2	3%
Platform	2	10.88	100
Sea knoll	7	1.97	100

Table 4-8-12 Relation Between Local Sea Floor Topography and Abundance of Manganese Nodules in Hilly Province

Topography	No. of sampling points	Average abundance	Occurrence ratio $\geqq 5\ kg/m^2$
Flat	15	9.36 kg/m^2	66.7%
Platform	6	4.09	16.7
Sea knoll	6	6.03	33.3

As shown in both tables, the data for platform and sea knoll are too limited. Comparison and examination were executed only on the flats; the values on the flat indicate an opposite tendency in case of those on plains and those on hills.

The average abundance for the flat on plains was low at 1.32 kg/m^2 with the occurrence ratio being only 3% of the area having an abundance of more than 5 kg/m^2. As for the sea knolls, the abundance and occurrence ratio were respectively high 9.36 kg/m^2 and 66.7%.

(3) SBP type and abundance

The relationship between the SBP type and abundance are shown in Fig. 4-8-20. As for the plains, the abundance of type b and e1 with upper transparent layers is lower than that of type c, ds and d2 without them. The weight factor [*1] indicates 1.52 to 1.72, differences by respective SBP type are not recognized.

On the hills, on the contrary, abundance decreases in the following order type b (10 kg/m^2) with upper transparent layers, d2 and ds, c (0.13 kg/m^2) without upper transparent layers. But the coverage by samples obtained is almost the same value, 40%, for type b, d2 and ds, it means that type b with upper transparent layers has a larger weight factor than other SBP types without them, that is to say, granular size of manganese nodules in type b is larger than the others.

As mentioned above, in comparison with type b for plains and that for hills the distribution situation of the manganese nodules is reversed, the former is nearly sterile and the latter is highly concentrated.

(4) Upper transparent layers and abundance

The relationship between the thickness of upper transparent layers and abundance is shown in Fig. 4-8-21.

---

*1 cf. Paragraph 4-4-(1)

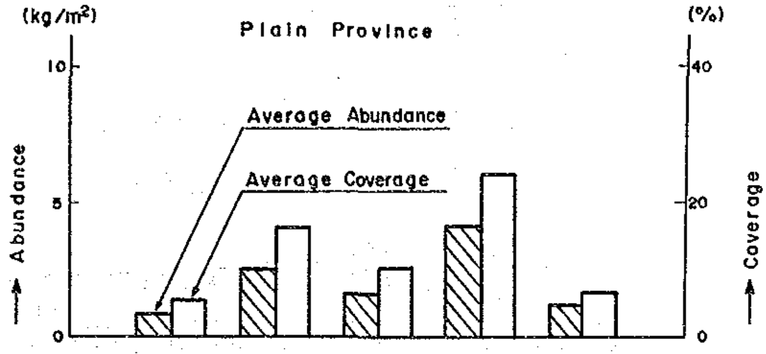

SBP Type	b	c	ds	d2	e1
Average Abundance	0.92	2.48	1.53	4.01	1.16
Average Coverage	5.67	15.84	10.06	23.95	6.74
Weight Coefficient	1.62	1.57	1.52	1.67	1.72
Number of Samples	37	18	14	6	5

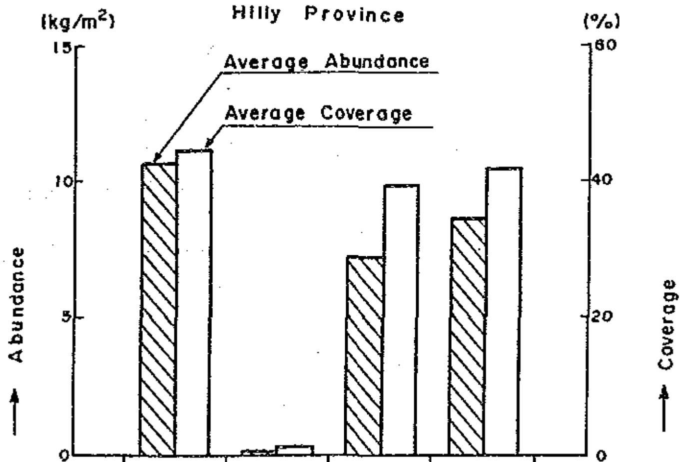

SBP Type	b	c	ds	d2
Average Abundance	10.51	0.13	7.18	8.64
Average Coverage	43.96	1.23	39.40	41.87
Weight Coefficient	2.39	1.06	1.82	2.04
Number of Samples	12	6	11	3

Fig. 4-8-20 Relation Between SBP Type and Abundance of Manganese Nodules

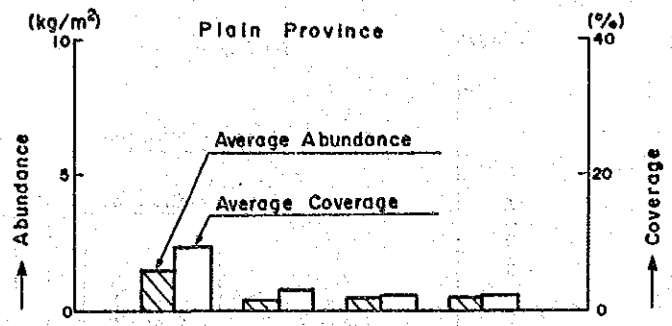

Transparent Layer	10.00	20.00	30.00	30 <
Average Abundance	1.48	0.42	0.46	0.51
Average Coverage	9.36	3.13	2.23	2.13
Weight Coefficient	1.58	1.34	2.06	2.39
Number of Samples	20	9	8	6

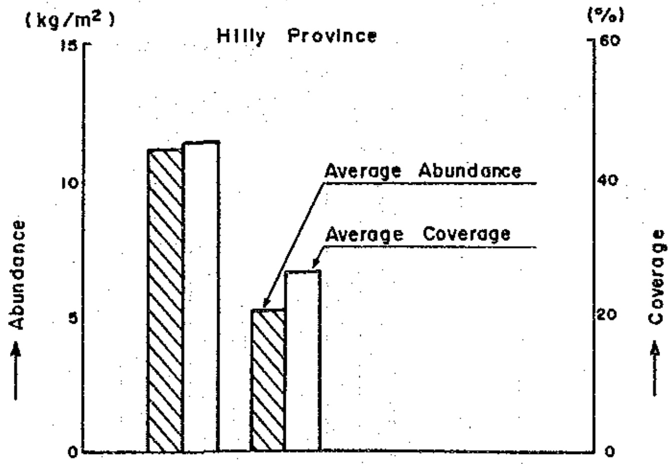

Transparent Layer	10.00	20.00	30.00	30 <
Average Abundance	11.15	5.05	—	—
Average Coverage	45.27	26.23	—	—
Weight Coefficient	2.46	1.93	—	—
Number of Samples	10	3	—	—

Fig. 4-8-21 Relation Between Upper Transparent Layer Thickness and Abundance of Manganese Nodules

Manganese nodules with upper transparent layers are only type b and e 1. Because of limited data, the correlation between the thickness of upper transparent layers and abundance was not found out, but as shown in 4-8-22, abundance has a tendency to become lower, as the thickness of the upper transparent layer increases, on both plains and hills.

(5) SBP Records and embedding ratio of the manganese nodules

In these low abundance areas, the manganese nodules of the embedded type are widely distributed, as shown in Fig. 4-4-2. The relationship between SBP records and the embedding ratio *1 are shown in Table 4-8-13.

Table 4-8-13 Relation Between Thickness of Upper Transparent Layers by SBP and Embedding Ratio

Layers' thickness	10 (m)	20	30	30 <
Embedding ratio	0.44	0.68	0.90	0.97
No. of samples	30	12	8	3

As this value grows larger, the embedding ratio increases. Cases where the grab collecting efficiency is less than 0.2, can be considered as exposed type.

As is evident from Table 4-8-13, as the thickness of the upper transparent layers increases, there is a tendency for the embedding ratio of the manganese nodules to become larger. Embedding ratio by respective SBP type are shown in Table 4-8-14.

---

*1 embedding ratio can be calculated by the following formula.
Embedding ratio = 1 - (photographic surfac ratio/re-collecting surface ratio)

Table 4-8-14 Relation Between SBP Type and Embedding Ratio of Manganese Nodules

Type of SBP	b	c	ds	d2	e1
Embedding ratio	0.42	0.76	0.70	0.52	0.86
No. of samples	49	24	25	9	6

From Table 4-8-14, in types b and e1 with upper transparent layers the embedded type of manganese nodules are largely observed; this is assumed according to the relation with layers thickness. But, while the type ds without upper transparent layers is the exposure type, type c and d2 are the embedded type. It is reasonable to assume that type c and d2 are on the plain and have a relatively thicker superficial sediment *1 than type ds. But the SBP records don't show transparent layers.

So it is assumed that superficial sediment is only a few meters in depth, even if there is any superficial sediment. The relationship between sea floor topography, SBP type and the thickness of upper transparent layers, indicates the areas where manganese nodules could be abundant. Examples of conditions mentioned above are as follows:

- the areas of flat on hills
- the areas with upper transparent layers with a thickness of about 10 m.

(6) Bottom materials and abundance

Fig. 4-8-22 shows the relation between bottom materials and abundance. Average abundance for the calcareous sediment is higher than that of the brown clays. As stated above, most of calcareous sediment exists near sea knolls.

---

*1 Superficial sediment corresponds to the upper transparent layers and quaternary sediment are collected from transparent layers of type b and e 1.

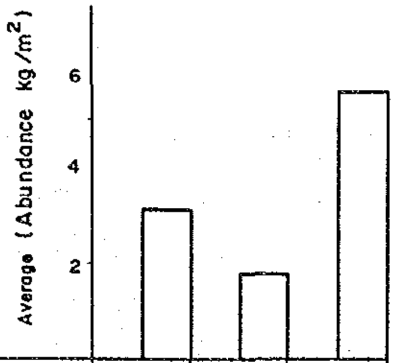

Bottom Setiments	Brown clay	Zeolitic clay	Calcareous sediment
Average (Abundance kg/m²)	3.17	1.78	5.58
Standard deviation	5.03	—	8.20
Number of samples	100	1	6

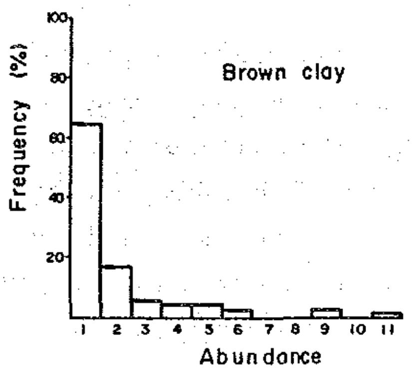

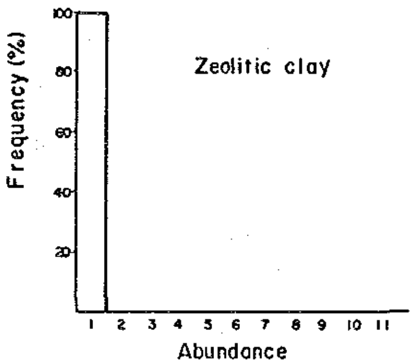

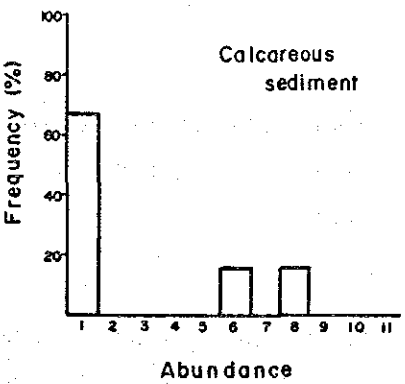

Legend

	Abundance
1	0 ~ 2.5 kg/m²
2	~ 5.0
3	~ 7.5
4	~ 10.0
5	~ 12.5
6	~ 15.0
7	~ 17.5
8	~ 20.0
9	~ 22.5
10	22.5~25.0
11	over 25.0kg/m²

Fig. 4-8-22 Average Abundance by Respective Bottom Sediments and Occurrence Ratio by Respective Abundance of Manganese Nodules

4-9 Bearing Situation of Manganese Nodules

1) Abundance of the manganese nodules (refer to annexed figure 7)

Looking at the distribution situation in general terms there are three sites where the average abundance is more than 5 kg/m^2. These three sites consisting of about 9% of the surface of the surveyed areas (85,000 km^2) are as follows;

① The site in western part demarcated by the 159°W along the western edges of the surveyed area from 5°30'S to 8°30'S with a peak point at 7°45'S: 159°15'W. (85-A)

② Insular site around the position 7°30'S: 158°30'W (85-B)

③ the semi circle site around the position 8°30'S: 158°30'W at southern edges of the surveyed areas. (85-C)

The western part demarcated by the line 159°W corresponds to the outside flank margin of the Manihiki plateau and presents a complex and intensively undulated topography. The eastern part demarcated by the line 159°W presents a plain bottom. Within this part, the isolated summits of sea knolls and sea mounts are dispersed along latitudial line 7°30'S to the east. The manganese nodules with flat and elliptical morphology and granular size less than 4 cm make up about 70%.

The surveyed areas could be considered as the areas where small size manganese nodules exist.

2) Grade distribution

In the surveyed areas, the metal content, could be considered to have areas where Ni and Cu contents are low and Co is high the following the general condition of Ni, Cu and Co contents:

(1) Ni content (cf. the annexed figure 8)

Ni content indicates a maximum of 1.34%, a minimum 0.13% and an average 0.74%. In general, the areas where the Ni content is high indicate a low abundance, as stated "4-8".

The areas with a abundance of less than 5 kg/m^2 corresponding to about 80% of the surveyed areas, indicate 0.5 - 1.29% Ni. Ni content where the abundance of manganese nodules is more than 5 kg/m^2 is as follows;

① 85-A: external margin of Manihiki plateau
surface: about 6,500 km^2
average Ni grade: 0.32%

② 85-B: insular site around the position 7°30'S: 158°30'W
surface: about 800 km^2
average Ni grade: 0.47%

③ 85-C: insular site around the position 8°30'S: 158°W
surface: about 400 km^2
average Ni grade: 0.27%

(2) Cu content (cf. the annexed figure 9)

Cu content indicates a maximum of 0.98%, a minimum of 0.09% and an average of 0.51%. The distribution situation of Cu content has the same tendency as Ni.

But the Cu content has little correlation with the abundant compared with Ni. There are some sampling points in areas with an abundance of less than 5 kg/m^2 which indicate a Cu content that is less than 0.5%.

① 85-A: Average Cu Content: 0.28%

② 85-B: Average Cu Content: 0.28%

③ 85-C: Average Cu Content: 0.17%

The areas where Cu content indicates more than 0.8% are the northern part of the middle area and south eastern area.

(3) Co content (cf. the annexed figure 10)

Co content indicates a maximum of 0.55%, a minimum of 0.10% and an average of 0.28%. In high abundance areas, Co content indicates high, compared with Ni and Cu content.

① Co content in the 85-A where the abundance is more than 5 kg/m^2 mostly indicates more than 0.35% and the average is 0.43%.

② Average Co content in the 85-B is 0.37%.

In southern part near 8°S in the middle of the surveyed area, where abundance is less than 5 kg/m^2, there are many points where Co content indicates more than 0.3%. Co content is 0.32%, although the average abundance of 6 sampling points in this area indicates 3.30 kg/m^2.

③ As for the average Co content in the 85-C, Ni and Cu contents become higher to the north of the 8°S line and Co becomes higher to the south of the 7°S line in eastern part demarcated by the 159°W.

(4) Mn and Fe content

Mn content indicates a maximum of 28.61%, a minimum of 2.23% and an average of 17.99%. Fe content indicates a maximum of 18.42%, a minimum of 4.99% and an average of 10.84%.

(5) Correlation between each components

Positive correlation is confirmed amongst Ni, Cu and Mn, and among Co and Fe. Among Ni-Cu-Mn and Co-Fe groups, reverse correlation is confirmed. Among abundance and nickel, reverse correlation is observed and among abundance and cobalt positive correlation is observed.

3) Distribution of metal quantity

Considering manganese nodules as useful ore reserve, it is necessary to consider not only the quantity of the manganese nodules per unit area, that is, high coverage but also the metal quantity included in the manganese nodules (specially Ni, Cu and Co that are useful metals).

For Ni, Cu and Co, the metal quantity per unit area is calculated for each sampling as in the following formulas with metal content value, and the results are described in annexed figures 13 - 15.

* Ni metal quantity per unit area = abundance x (1-water content) x Ni grade
* Cu = abundance x (1-water content) x Cu grade
* Co = abundance x (1-water content) x Co grade

In this case, a cut off grade for each metal is not used. As stated later, the characteristics of distribution of metal quantity in the surveyed area is that the area where Ni, Cu and Co contents are high indicates high abundance of manganese nodules.

(1) Ni (cf. annexed figure 13)

As shown in this figure, the areas with more than 20 g/m^2 (Ni) are the following four;

- the site between the 159°W and the line 159°30'W which is the west end of the surveyed areas.
- the insular site around the position of 7°30'S: 158°30'W.
- the insular site around the position of 8°00'S: 157°00'W.
- the site around the position 6°30'S: 156°30'W.

In the surveyed areas, the total surface area where Ni content indicates more than 20 g/m^2 is about 7,500 km^2 and the average content is 29.2 g/m^2.

(2) Cu (cf. annexed figure 14)

As shown in this figure, the areas where Cu content indicates more than 20 g/m^2 are generally similar with Ni, but these are limited because of lower grades.

In the surveyed areas, the total surface area where Cu content indicates more than 20 g/m^2 is about 630 km^2 and the average contnt is 23.2 g/m^2.

(3) Co (cf. annexed figure 15)

As shown in this figure, the areas where Co content indicates more than 10 g/m^2 are similar to the areas where Ni content indicates more than 20 g/m^2. In the surveyed area, the total surface area where Co content indicates more than 10 g/m^2 is about 8,340 km^2 and the average content is 29.0 g/m^2.

Chapter 5. Summary

1) Conclusion

Comparing the sea floor topography with the distribution of manganese nodules, the bearing situation of the deep-sea ore resources were characterized by the sea depth and the sea floor topography. In the surveyed areas, especially in the Plain Province, ore resources might be rare until the depth reaches around 4,000 m, if any, they were less than 5 kg/m^2.

Though there observed some crustic-type mineral deposits at depth between approximately 4,000 and 4,500 m, the majority were basement rock and rockmass which were exposed.

At a depth range of around 4,500 to 5,100 m, the most prominent mineral resources observed were crust-type and some manganese nodules in limitted areas.

At a depth range of around 5,100 to 5,600 m, manganese nodules were generally abundant.

In the eastern part demarcated by the line 159°W, the Plain Province of the surveyed areas, at a depth range of around 5,100 to 5,400 m, the abundance of manganese nodules were comparatively moderate. Below a depth of 5,400 m, the abundance of manganese nodules decreased. And it might be less than 3 kg/m^2 at most and the average is less than 1 kg/m^2.

Topographically, the concentrated areas of manganese nodules were observed in areas of the complex Hilly Province mainly at the external margin of the Manihiki plateau. Almost nothing was observed on the plain.

(1) Sea floor topography

The sea floor topography showed a trend of deepening toward the west of the longitudinal line 157°30'W and getting shallower toward the east of that line.

The eastern part demarcated by the line 159°W presented mostly plain bottom. Within this part, the isolated summits of sea knolls and sea mounts were dispressed along the laditudinal line 7°30'S. And massive isolated sea mounts with relative heights of 1,200 m were recognized around the position 7°30'S: 157°30'W.

The western part demarcated by the line 159°W corresponded to the external margin of the Manihiki plateau which covers an extensive area, and presented a coxlex and intensively undulated topography.

(2) Distribution of manganese nodules

The abundance of manganese nodules in the surveyed areas was ascertained, in general, higher to the west of the longitudinal line 158°W and lower to the east.

The following three areas were confirmed to indicate an abundance of more than 5 kg/m^2:

① 85-A: external margin of the Manihiki plateau in western part demarcated by the line of 159°W
surface: about 6,500 km^2

② 85-B insular site round the position 7°30'S: 158°30'W
surface: about 800 km^2

③ 85-C: insular site round the position 8°30'S: 158°30'W
surface: about 400 km^2

The sea floor of these areas showed to be quite undulated and the depth measured was some 5,100 - 5,600 m.

Exposure ratio of manganese nodules was rather high.

Throughout almost all the surveyed areas, especially around the sea mounts or sea knolls where the sea depth is less than 5,000 m, manganese nodules were found, in the state of plate, crust or massive rocks. In rare cases, it was observed that basement rock was exposed directly.

(3) Bottom materials

The sea floor of almost all the areas surveyed were covered with brown clays. Calcareous clay was observed slightly only near the summits of sea mount or sea knolls where the sea depth was less than 5,000 m. Also, in extremely rare cases, clay rich in zeolite was observed within the limits of brown clay distribution areas. On the basis of the present survey data, no correlation between the bottom materials and the manganese nodules were able to be confirmed.

2) Grade distribution and metal quantity distribution of manganese nodules

As for the grade and distribution of the metal quantity of the manganese nodules in the surveyed areas, the following regularity was ascertained:

(1) Grade distribution

Concerning the three components nickel, copper and cobalt that are significant metal of manganese nodules in the surveyed areas, the followings were observed:

① The average for whole surveyed areas;

Ni grade was 0.74%, Cu 0.51% and Co 0.28%;

② Concerning the areas where the abundance of manganese nodules was more than 5 kg/m^2, Ni and Cu grades tended to decrease, while Co tended to increase as follows;

Ni: 0.44%, Cu: 0.27% and Co: 0.39%;

③ As for the areas where the abundance was more than 7.5 kg/m^2, Ni and Cu grades were found at the same level but the Co increased rather high.

The surveyed area could be considered to have areas where Co grade be relatively high.

(2) Distribution of metal quantity

Concerning the three components nickel, copper and cobalt mainly useful elements of manganese nodules in the surveyed areas, the metal quantity per unit area were as follows;

① The surface area where Ni metal quantity was more than 20 g/m^2 was about 7,500 km^2 and average metal quantity indicated 29.2 g/m^2.

② The surface area where Cu metal quantity was more than 20 g/m^2 was about 630 km^2 and average metal quantity indicated 23.2 g/m^2.

③ The surface area where Co metal quantity was more than 10 g/m^2 was abut 8,340 km^2 and average metal quantity indicated 29.0 g/m^2.

3) Proposal for the next financial year

As the next steps in surveying the manganese nodules we propose the following:

(1) To proceed a topographical survey of the sea floor by the echo sounder in the area that locate to the southwest part of the currently surveyed area; and

To determine potential sea areas by means of the primary and secondary samplings with a grid of 42.4 and 21.2 nautical miles;

(2) To select an adequate measuring line; and

To confirm the continuance of the distribution of manganese nodules by means of CDC.

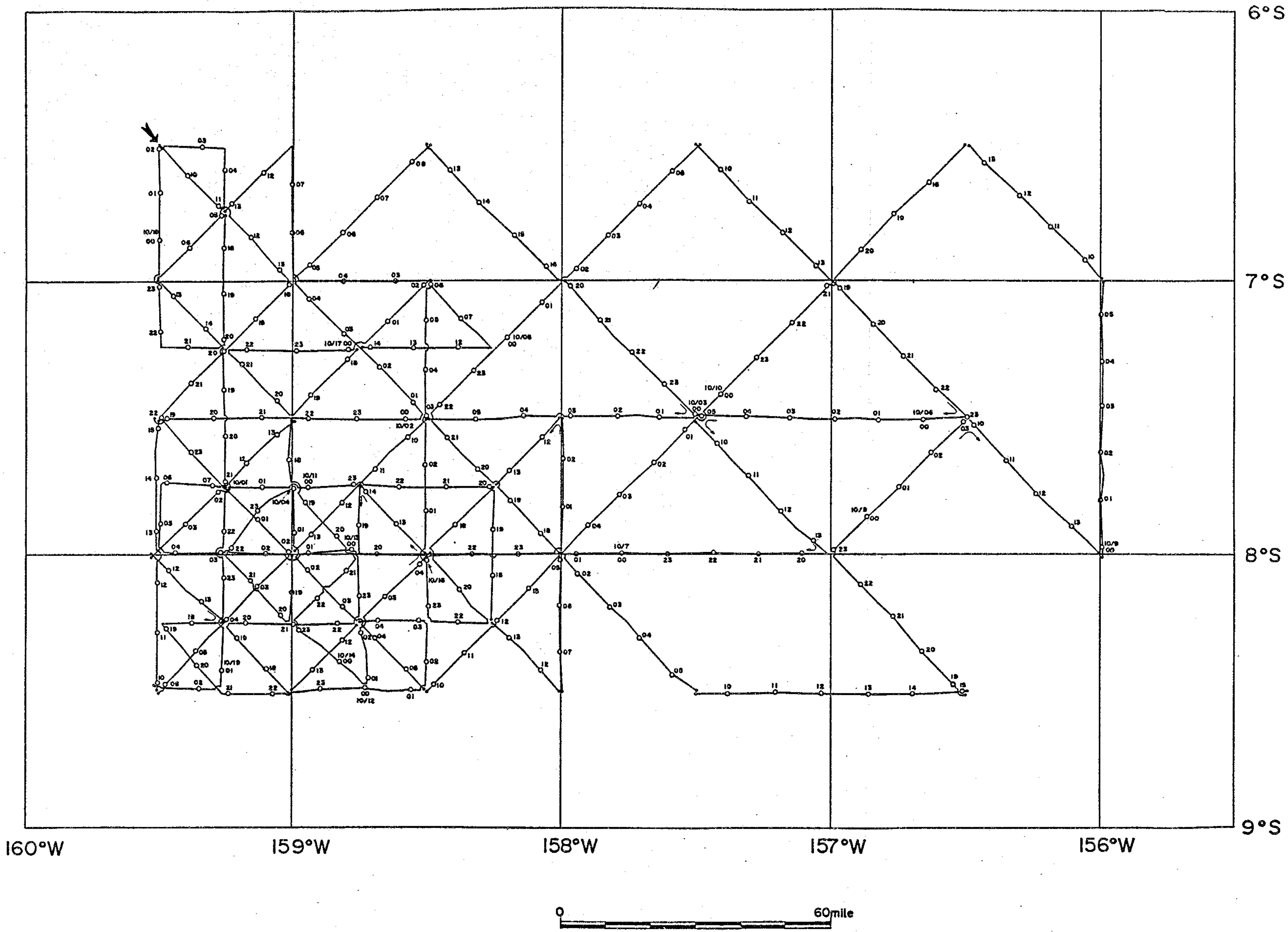

Annexed Figure 1 Tracklines Map

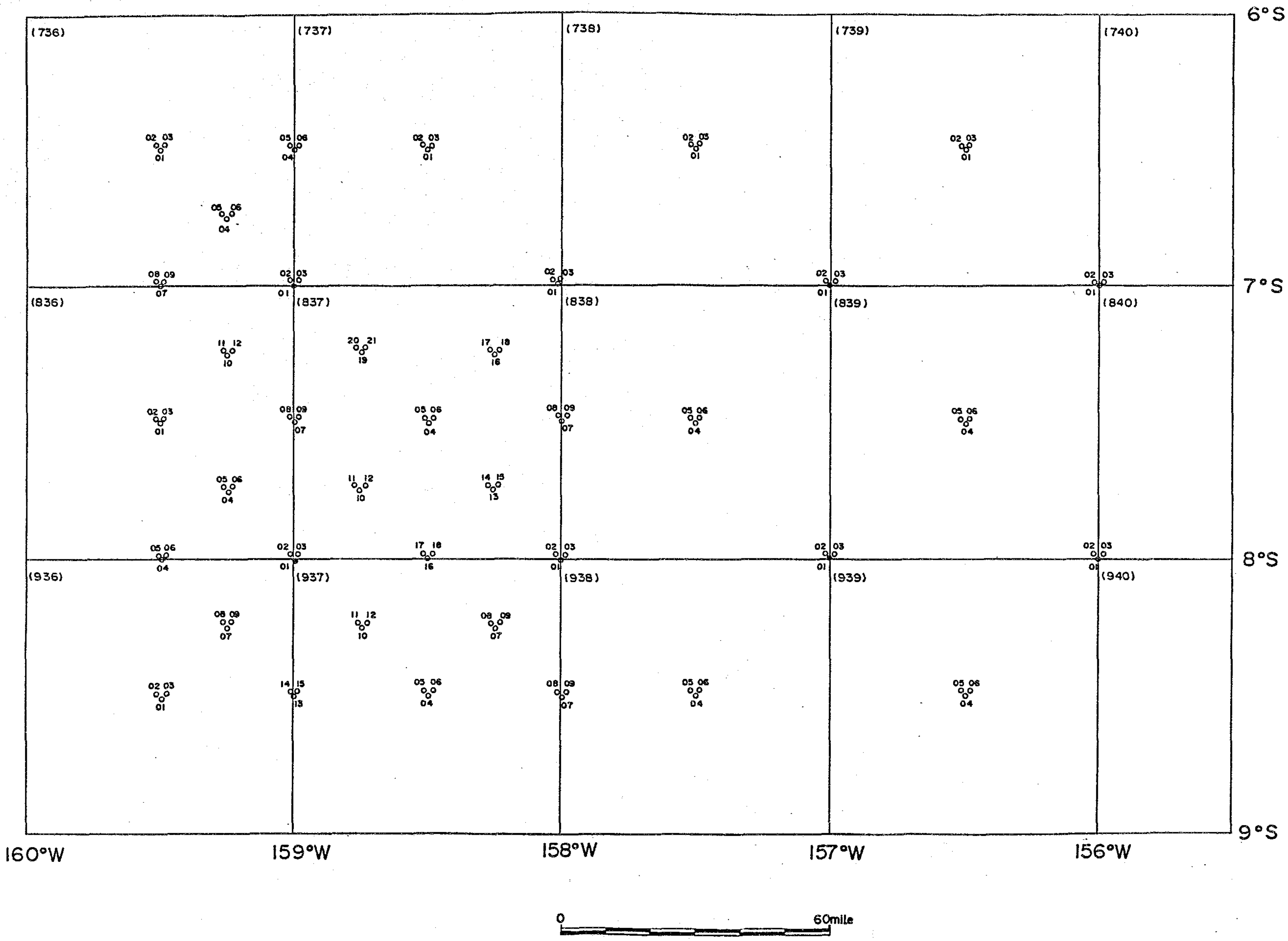

Annexed Figure 2 Positions of Sampling Points

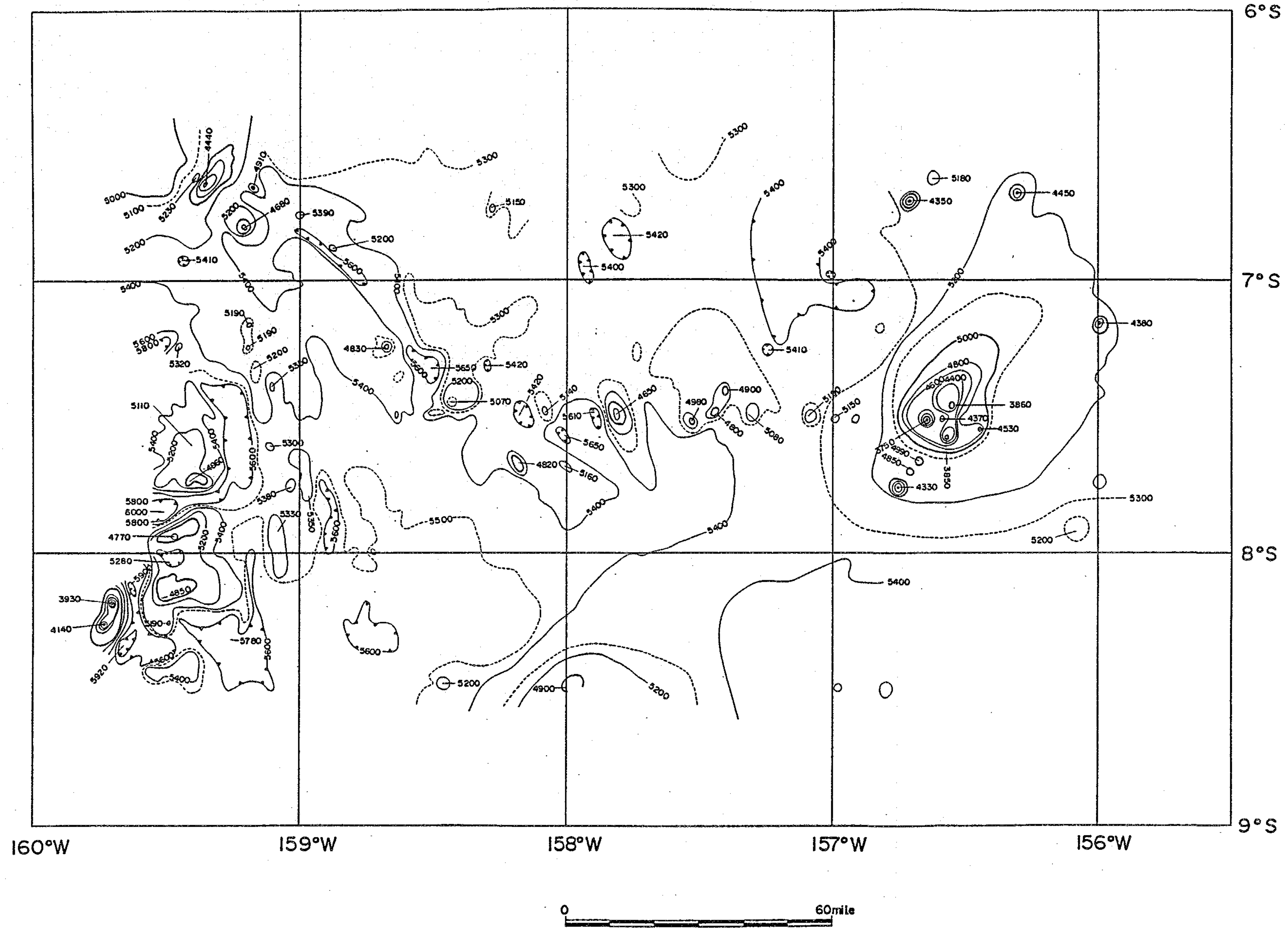

Annexed Figure 3 Sea Floor Topography

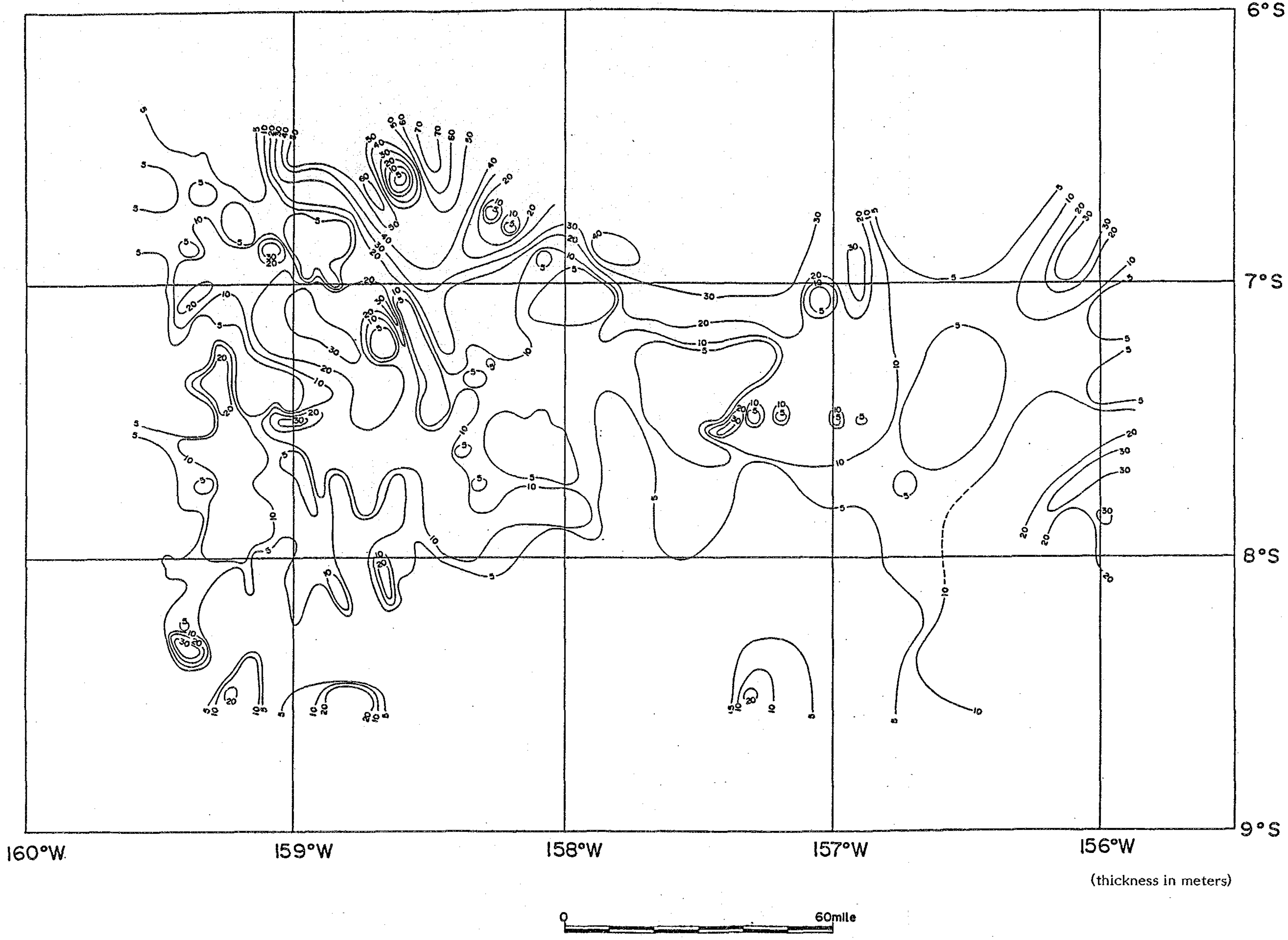

Annexed Figure 4 Acoustic Thickness of Upper Transparent Layers by SBP

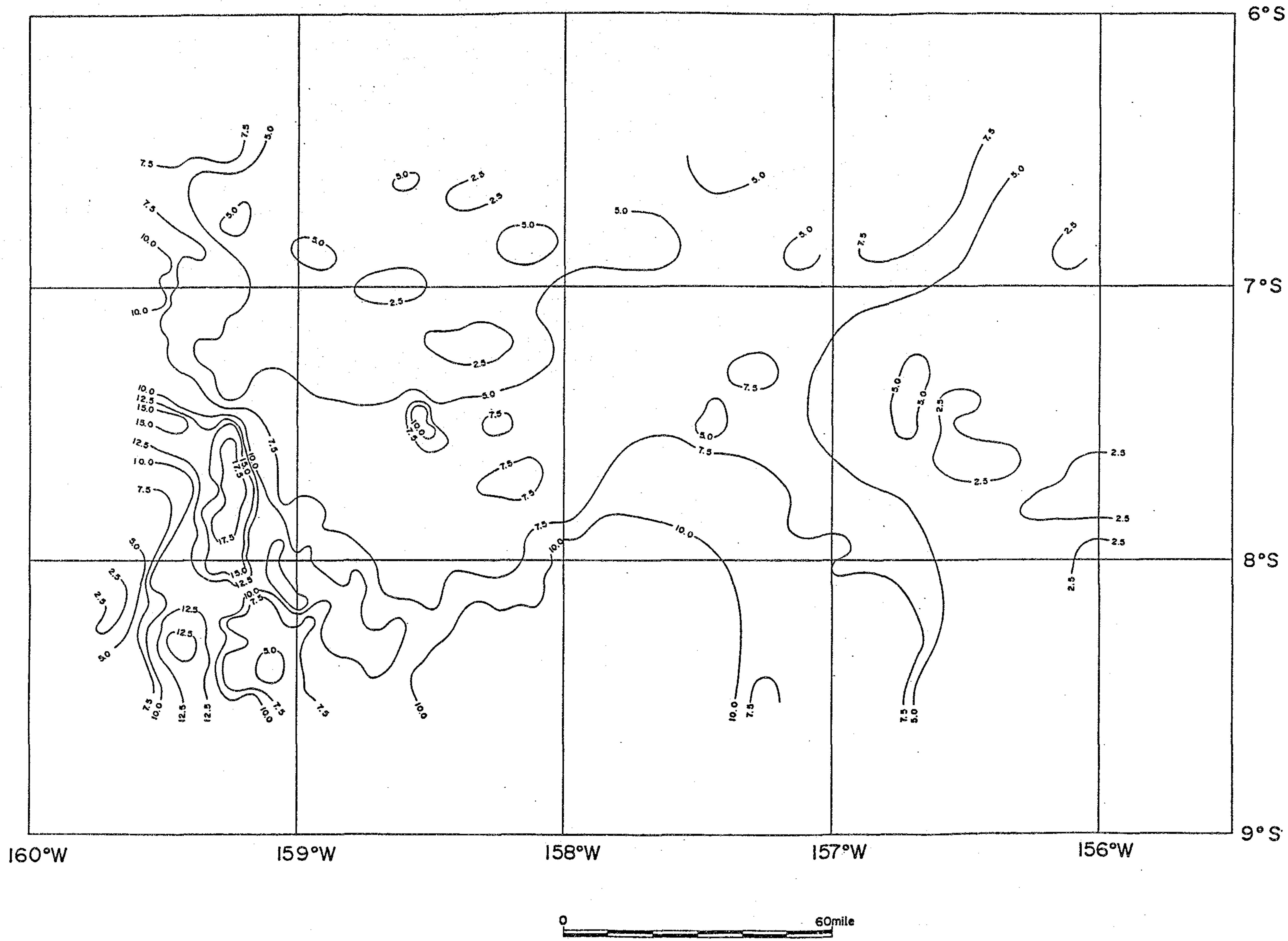

Annexed Figure 5 MFES Intensity Map

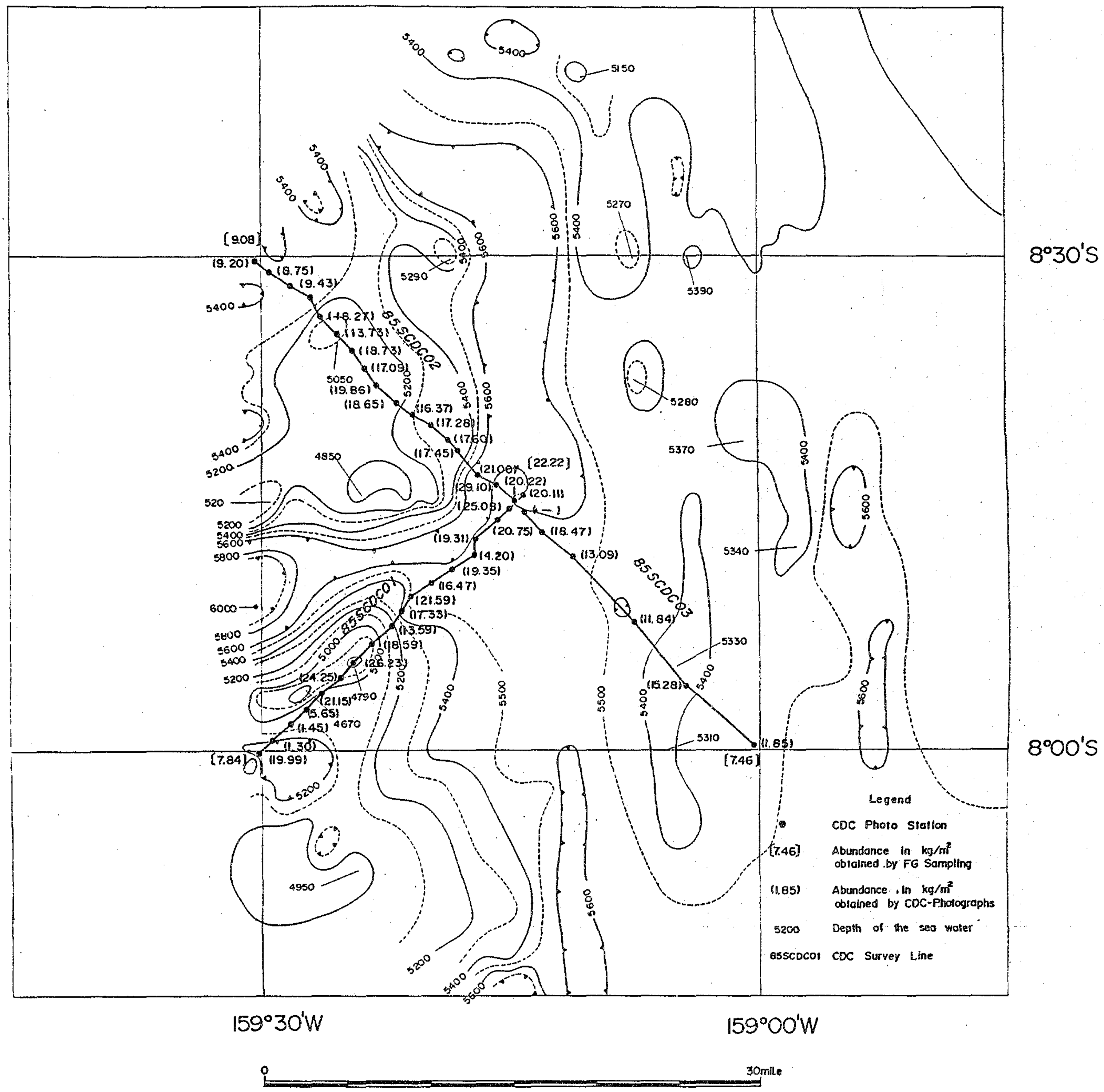

Annexed Figure 6 Estimated Abundance by CDC Observation

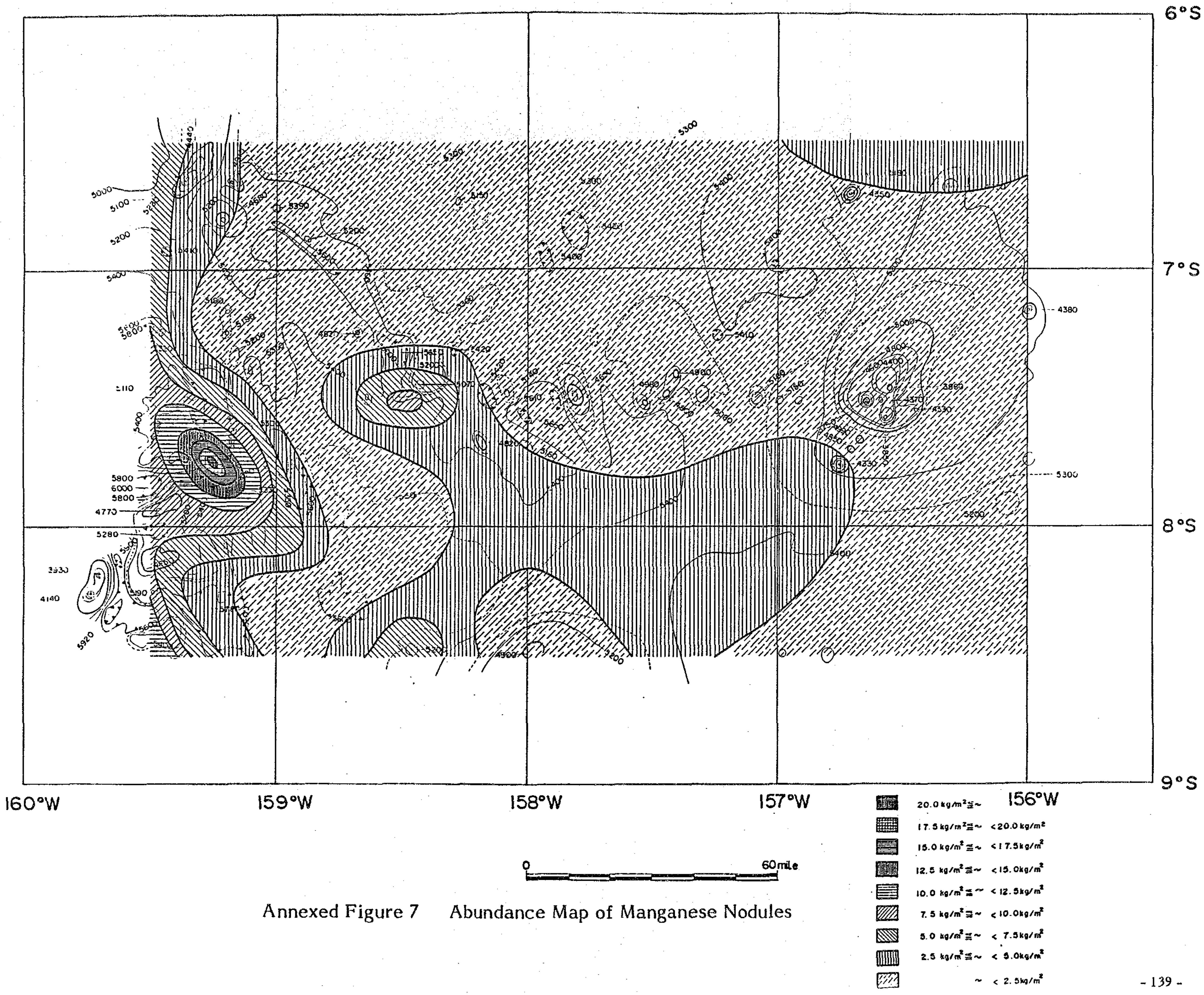

Annexed Figure 7 Abundance Map of Manganese Nodules

Annexed Figure 8 Ni Grade Map of Manganese Nodules

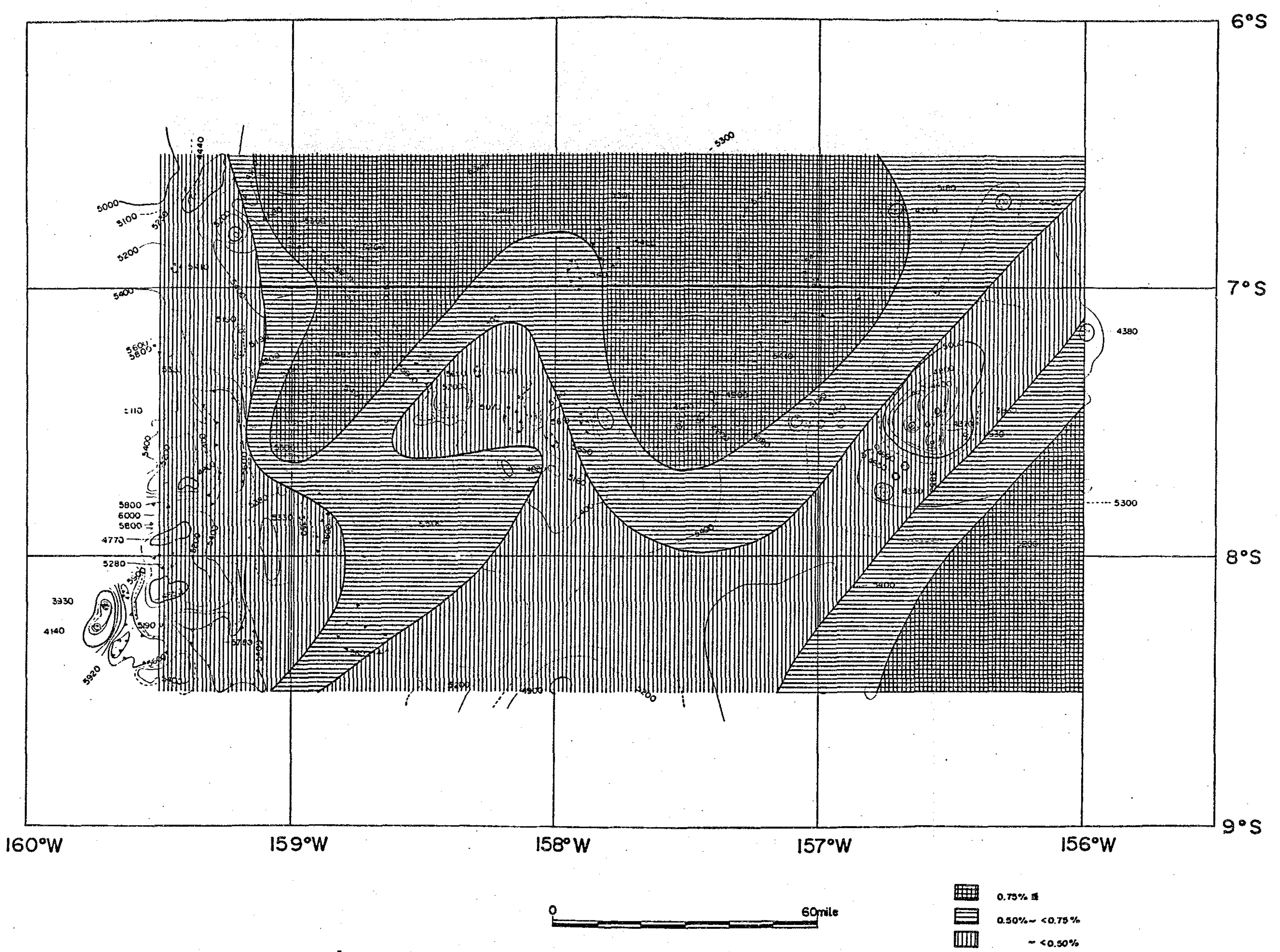

Annexed Figure 9 Cu Grade Map of Manganese Nodules

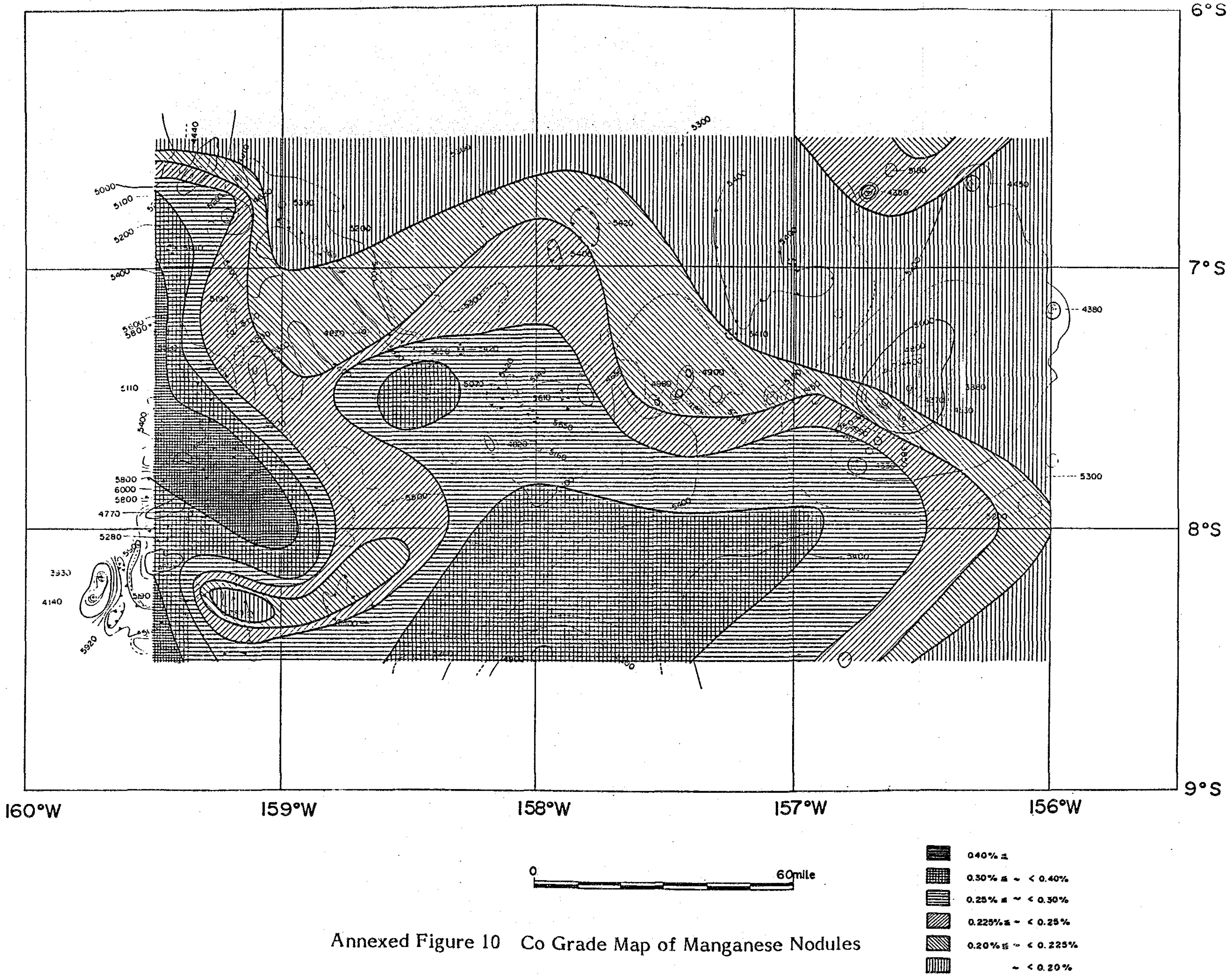

Annexed Figure 10 Co Grade Map of Manganese Nodules

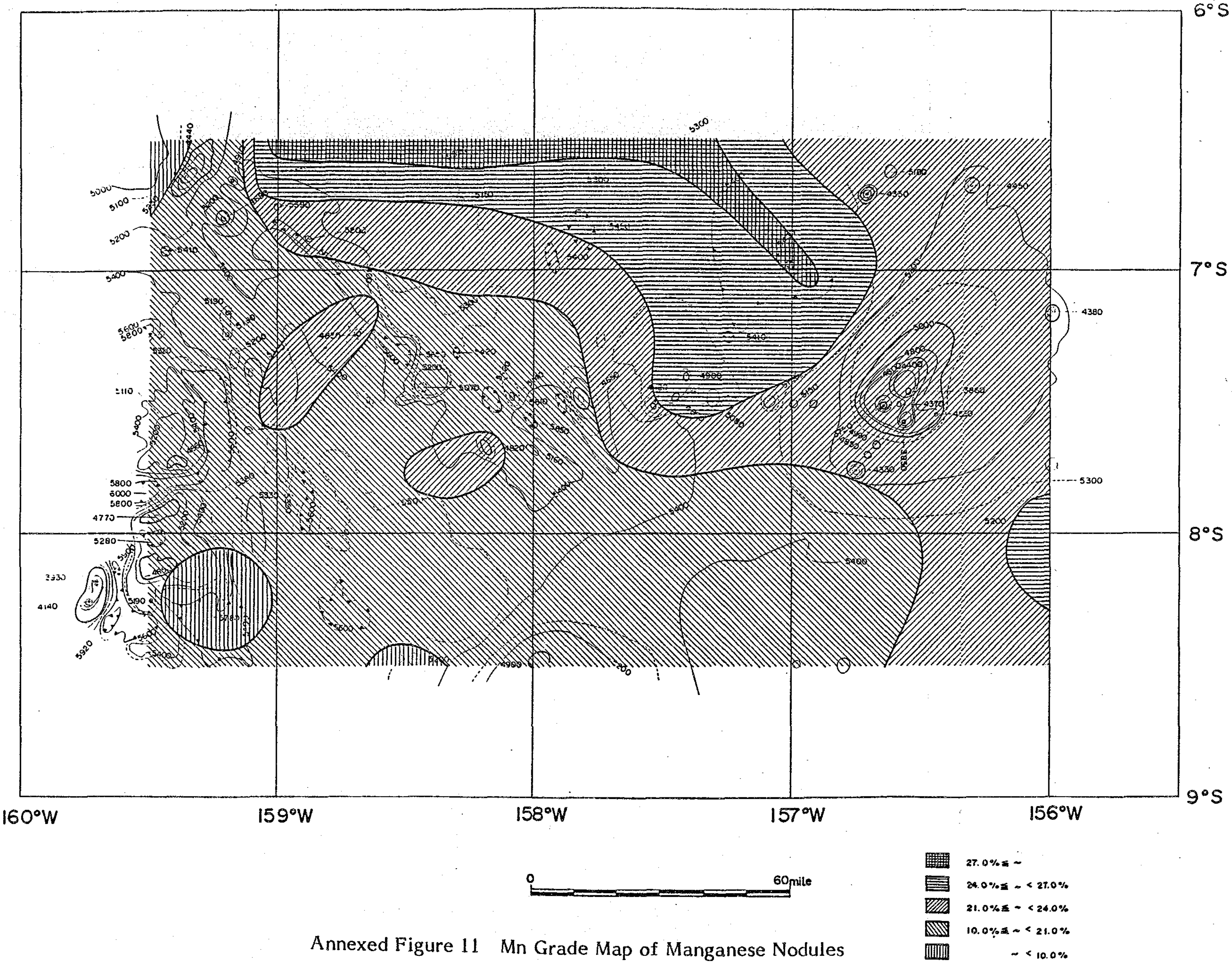

Annexed Figure 11 Mn Grade Map of Manganese Nodules

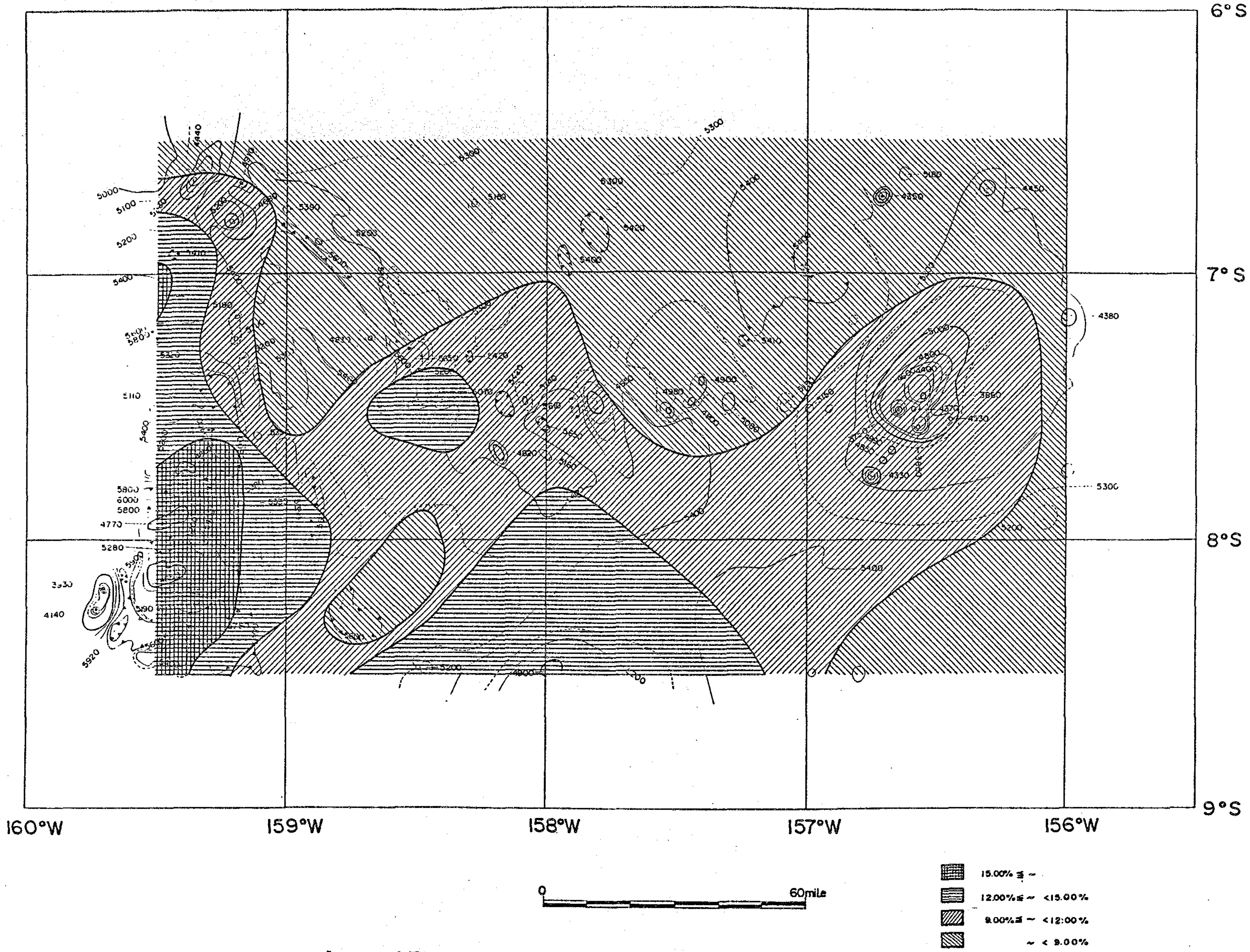

Annexed Figure 12 Fe Grade Map of Manganese Nodules

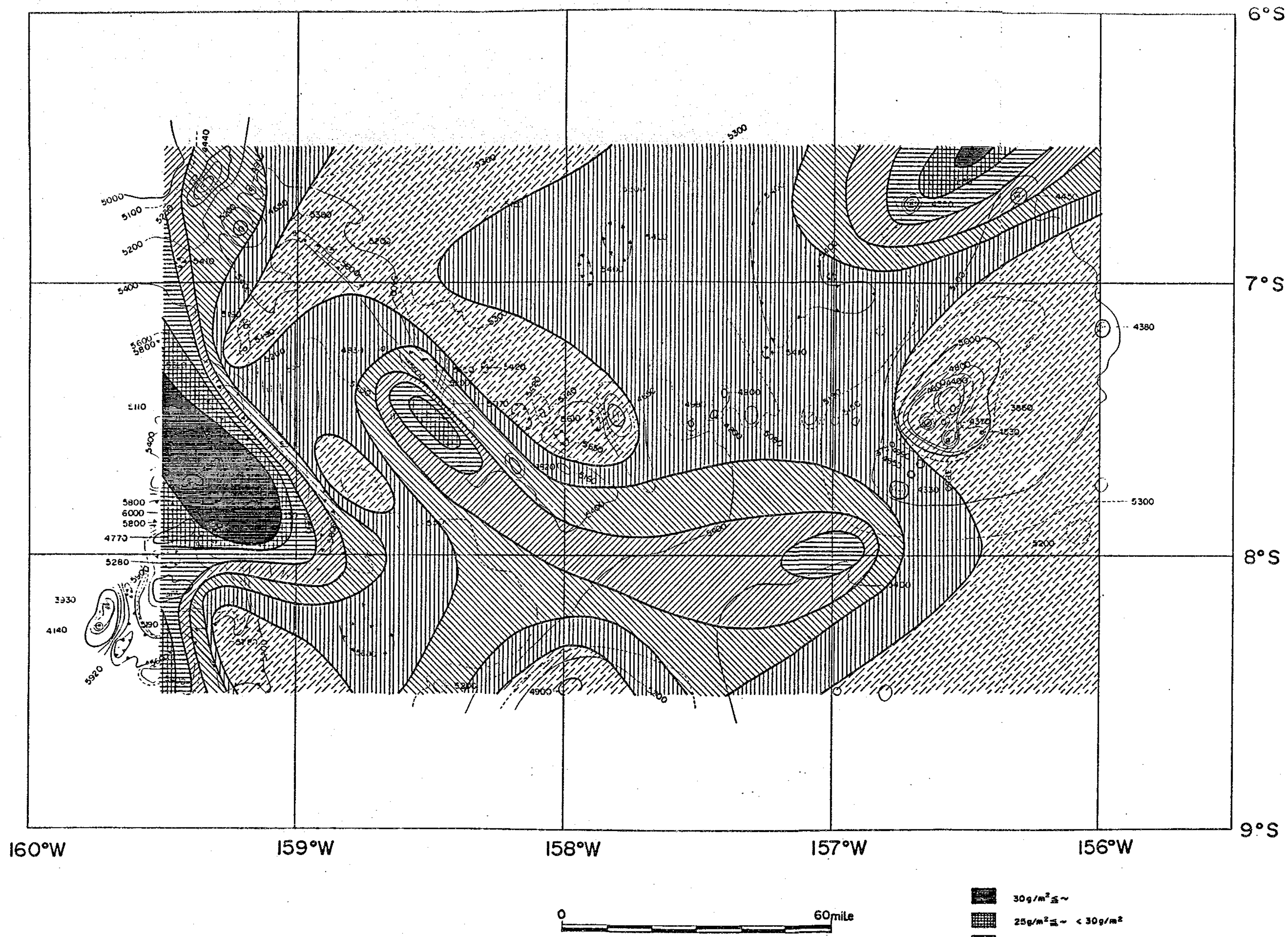

Annexed Figure 13 Ni Metal Quantity Map

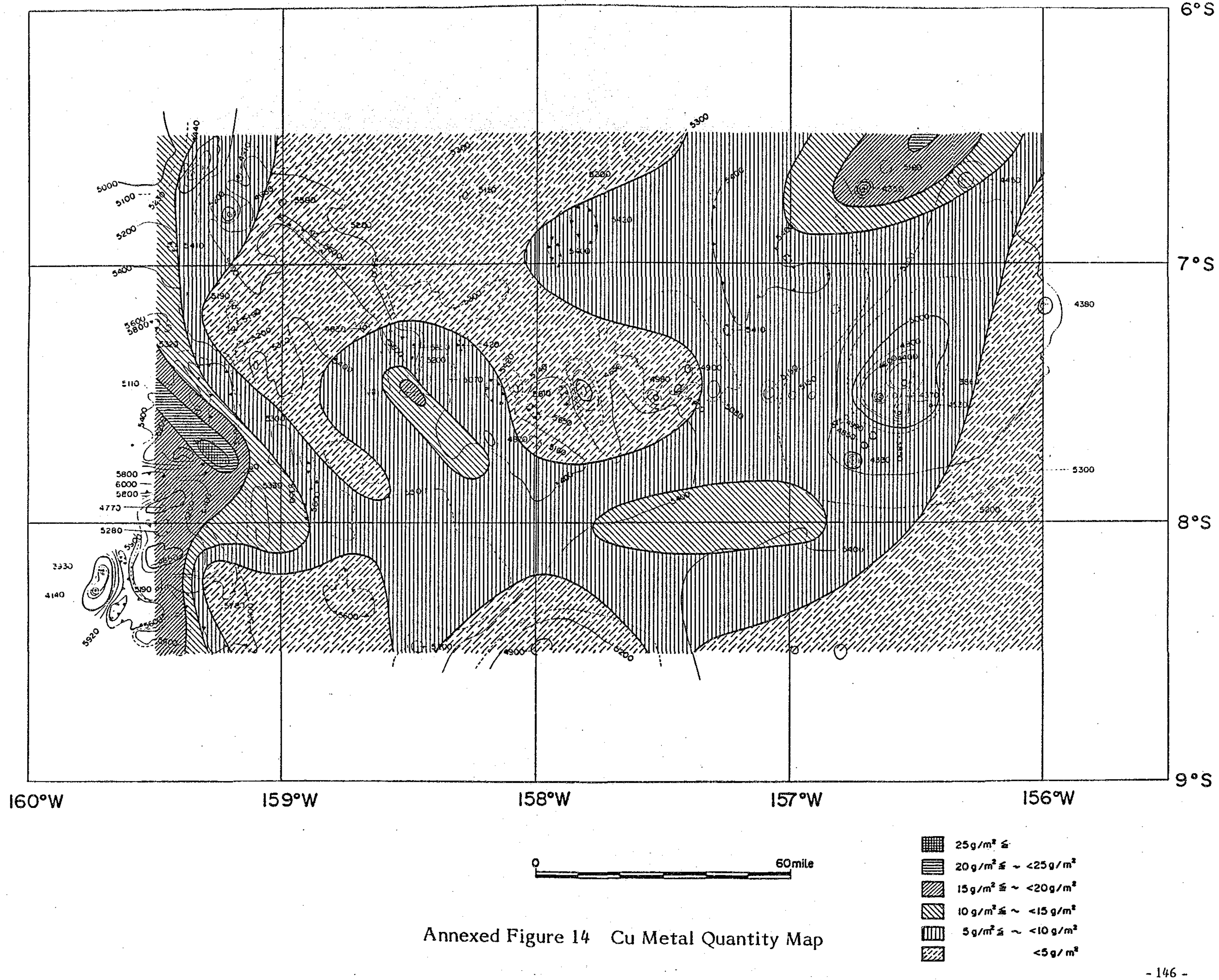

Annexed Figure 14 Cu Metal Quantity Map

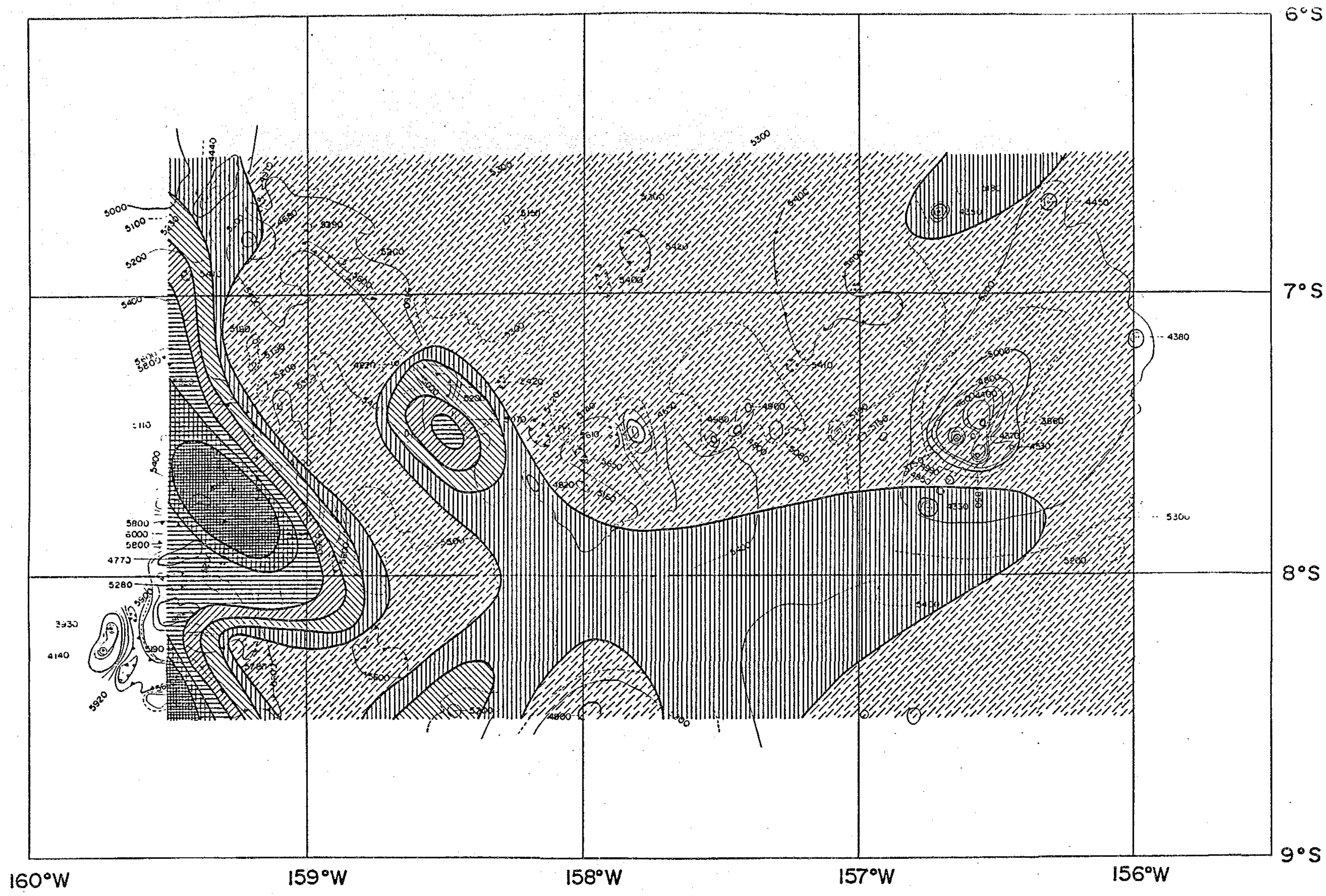

Annexed Figure 15 Co Metal Quantity Map

Data file around the Cook Islands

(No. 1)

Sample No (Station)	Location: Latitude	Longitude	Depth (m)	Topography	Manganese Nodules: Size distribution (%) 0-2 cm	2-4 cm	4-6 cm	6-8 cm	8-16 cm	16- cm	Abundance (Kg/m2)	Shape	S.G. wet	H2O (%)	XRF Analyses (%) Ni	Cu	Co	Mn	Fe	Geology: Sediment	T.P.L.* type	T.P.L.* thick. (m)	Remarks
85S736FC01	06° 30.07'S	159° 30.18'W	4.944	(Mo) fl	20	11	29	16	24		8.27	N.Pl	2.00	28.4	0.37	0.29	0.10	3.56	8.72	BC	b	20	
85S736FC02	06° 29.01'S	159° 31.02'W	4.944	(Mo) fl	25	26	1		48		5.57	Pl.Ot	2.05	24.4	0.54	0.32	0.21	9.02	7.98	BC	b	20	
85S736FC03	06° 29 07'S	159° 29.27'W	4.958	(Mo) fl	86	12	2				2.74	Ot.E	2.12	18.8	0.51	0.33	0.16	7.25	7.44	BC	d2	0	
(85S01) Average					33	18	15	6	28		5.53	Pl.N	2.04	25.4	0.45	0.31	0.15	8.09	8.24				
85S837SC01	07° 00.25'S	159° 00.01'W	5.390	(Mo) fl	75	25					0.58	Sp.E	2.05	22.5	1.02	0.68	0.19	18.74	7.69	BC	b	20	
85S837FC02	06° 59.04'S	159° 00.94'W	5.452	(Mo) fl	57	43					0.28	Sp.E	—	—	—	—	—	—	—	BC	a	5	
85S837FC03	06° 58.99'S	158° 58.96'W	5.353	(Mo) fl	71	18	11				0.88	E.Sp	2.16	21.7	1.14	0.76	0.20	20.69	7.51	BC	b	10	
(85S02) Average					70	24	6				0.58	Sp.E	2.12	22.0	1.09	0.73	0.20	19.92	7.58				
85S936FC01	08° 30.50'S	159° 29.80'W	5.551	(Mo) fl	2	51	31	12	4		20.94	E	2.10	28.3	0.35	0.23	0.46	17.78	16.91	BC	d2	0	
85S936FC02	08° 29.61'S	159° 30.73'W	5.510	(Mo) fl	0	10	47		43		5.16	El.Sp	1.94	32.8	0.13	0.12	0.55	17.42	16.28	BC	ds	0	
85S936FC03	08° 29.66'S	159° 28.78'W	5.474	(Mo) fl	7	66	22	5			8.43	E.Pl	1.91	31.8	0.37	0.23	0.37	11.93	15.43	BC	ds	0	
(85S03) Average					3	49	31	8	9		11.51	E.El	2.08	29.8	0.32	0.22	0.45	16.33	16.47				
85S836FC01	07° 30.10'S	159° 30.05'W	5.281	(Mo) hi	10	78	12				12.20	E.Pt	2.01	26.2	0.52	0.32	0.41	17.34	14.27	BC	ds	0	
85S836FC02	07° 29.18'S	159° 31.04'W	5.060	(Mo) hi	11	84	3	2			13.18	Pt.E	2.05	27.6	0.45	0.28	0.47	18.24	15.86	CSC	ds	0	
85S836FC03	07° 29.24'S	159° 29.18'W	5.425	(Mo) hi	18	68	14				1.78	E.Pl	2.10	24.1	0.68	0.37	0.30	14.98	11.43	ZC	ds	0	
(85S04) Average					11	80	8	1			9.08	E.Pt	2.04	26.7	0.50	0.31	0.43	17.66	14.84				
85S737FC01	06° 30.03'S	158° 30.04'W	5.269	(Pl) fl	60	40					0.12	Sp.E	—	—	—	—	—	—	—	BC	b	60	
85S737FC02	06° 29.15'S	158° 31.12'W	5.277	(Pl) fl	17	83					0.83	E.Sp	2.06	22.9	1.09	0.98	0.17	28.08	6.92	BC	b	50	
85S737FC03	06° 29.13'S	158° 29.36'W	5.292	(Pl) fl	24	76					0.25	E.Sp	—	—	—	—	—	—	—	BC	b	80	
(85S05) Average					24	76					0.33	E.Sp	2.06	22.9	1.09	0.98	0.17	28.08	6.92				
85S838FC01	06° 59.74'S	158° 00.96'W	5.383	(Pl) fl	88	12					0.12	Sp.E	—	—	—	—	—	—	—	BC	b	10	
85S838FC02	06° 58.80'S	158° 02.09'W	5.381	(Pl) fl	65	35					0.58	E.Sp	2.23	24.5	1.25	0.82	0.21	22.78	7.58	BC	b	10	
85S838FC03	06° 58.70'S	158° 00.31'W	5.369	(Pl) fl	49	45	6				2.33	E.Sp	2.09	27.0	0.99	0.65	0.25	21.01	9.34	BC	ds	0	
(85S06) Average					54	42	5				1.01	E.Sp	2.12	26.5	1.05	0.69	0.24	21.38	8.98				

* T.P.L : Transparent Layer

Data file around the Cook Islands

(No. 2)

Sample No. (Station)	Location				Manganese Nodules: Size distribution (%)						Abun-dance (Kg/m2)	Shape	S.G. wet	H2O (%)	XRF Analyses (%)					Geology			Remarks
	Latitude	Longitude	Depth (m)	Topography	0-2 cm	2-4 cm	4-6 cm	6-8 cm	8-16 cm	16- cm					Ni	Cu	Co	Mn	Fe	Sediment	T.P.L.* type	T.P.L.* thick (m)	
8SS837FC04	07° 30.05'S	158° 29.93'W	5,280	(Pl) ta	14	41	30	15			12.48	Pt.M	1.99	28.3	0.37	0.22	0.44	17.25	15.11	BC	b	5	
8SS837FC05	07° 29.14'S	158° 30.88'W	5,471	(Pl) fl	72	28					1.86	Sp.Pl	2.06	21.7	0.63	0.41	0.21	11.76	9.24	BC	ds	0	
8SS837FC06	07° 29.09'S	158° 28.91'W	5,321	(Pl) ta	20	57	16	7			9.29	Pt.E	2.08	28.8	0.57	0.34	0.32	15.13	12.75	BC	ds	0	
(85507) Average					21	46	22	11			7.87	Pt.M	2.03	27.2	0.47	0.28	0.37	15.95	13.68				
8SS937SC01	08° 00.13'S	159° 00.12'W	5,415	(Mo) fl	5	47	33	15			8.82	Pt.M	1.87	26.6	0.44	0.27	0.42	18.18	14.52	IBC/BC	b	5	
8SS937FC02	07° 59.11'S	159° 00.85'W	5,444	(Mo) fl	92	8					0.68	Sp.E	2.06	23.8	0.64	0.43	0.23	12.22	9.22	BC	b	10	
8SS937FC03	07° 59.15'S	158° 59.01'W	5,443	(Mo) fl	2	40	40	18			12.68	M.Pt	1.98	28.6	0.45	0.27	0.42	18.19	13.78	BC	b	5	
(85508) Average					7	42	38	18			7.48	M.Pt	1.97	27.6	0.45	0.27	0.41	17.94	13.88				
8SS937FC04	08° 29.93'S	158° 29.92'W	5,395	(Pl) hi	41	57	2				3.18	Pt	1.89	29.0	0.25	0.17	0.21	5.52	12.70	BC	ds	0	
8SS937FC05	08° 28.91'S	158° 30.81'W	5,490	(Pl) hi	23	43	24	10			8.42	E.M	1.93	34.0	0.27	0.17	0.35	11.45	15.03	BC	c	0	
8SS937FC06	08° 28.71'S	158° 28.78'W	5,157	(Pl) hi							(0.00)	—	—	—	—	—	—	—	—	-	ds	0	Sampling failed
(85509) Average					28	47	18	7			5.80	Pl.E	1.92	32.6	0.27	0.17	0.31	9.74	14.36				
8SS938FC01	08° 00.04'S	158° 00.10'W	5,423	(Pl) fl	71	29					3.88	Sp.E	2.03	27.1	0.65	0.40	0.31	17.03	11.75	BC	c	0	
8SS938FC02	07° 59.13'S	158° 01.14'W	5,431	(Pl) fl	46	54					3.74	Pl.Sp	1.88	28.8	0.81	0.38	0.36	19.24	13.27	BC	c	0	
8SS938FC03	07° 59.11'S	157° 59.30'W	5,418	(Pl) fl	79	21					1.84	Sp.E	2.04	24.2	0.73	0.46	0.29	17.50	11.17	BC	c	0	
(85510) Average					63	37					3.15	Sp.E	2.01	26.4	0.65	0.40	0.33	17.99	12.23				
8SS738FC01	06° 30.03'S	157° 30.02'W	5,283	(Pl) fl	15	41	44				0.61	E.Sp	—	—	—	—	—	—	—	BC	b	30	
8SS738FC02	06° 29.12'S	157° 31.06'W	5,272	(Pl) fl	100						0.01	E	—	—	—	—	—	—	—	BC	b	30	
8SS738FC03	06° 29.08'S	157° 29.20'W	5,254	(Pl) fl	6	68	26				1.46	E.Sp	2.12	26.3	1.06	0.95	0.17	28.61	6.86	BC	b	30	
(85511) Average					9	60	31				0.69	E.Sp	2.12	26.3	1.06	0.95	0.17	28.61	6.86				
8SS839SC01	07° 00.00'S	157° 00.27'W	5,400	(Pl) fl	8	92					1.22	E.Sp	2.12	27.7	1.14	0.93	0.19	27.03	7.55	BC	b	10	
8SS839FC02	06° 59.08'S	157° 00.95'W	5,396	(Pl) fl	36	64					0.81	E.Sp	2.10	23.1	1.17	0.93	0.18	27.26	7.05	BC	b	30	
8SS839FC03	06° 59.07'S	156° 59.02'W	5,396	(Pl) fl	7	69	24				1.18	E.Sp	1.98	25.0	1.12	0.92	0.18	27.40	7.46	BC	b	20	
(85512) Average					15	76	9				1.07	E.Sp	2.06	25.6	1.14	0.93	0.18	27.23	7.39				

* T.P.L. - Transparent Layer

Data file around the Cook Islands

(No 3)

Sample No. (Station)	Location: Latitude	Longitude	Depth (m)	Topography	Size distribution (%): 0-2 cm	2-4 cm	4-6 cm	6-8 cm	8-16 cm	16- cm	Abundance (Kg/m2)	Shape	S.G. wet	H2O (%)	XRF Analyses (%): Ni	Cu	Co	Mn	Fe	Geology: Sediment	T.P.L.*: type	thick (m)	Remarks
85S838FG04	07° 30.04'S	157° 30.05'W	5.251	(P I) f l	43	30	27				0.63	E.Sp	2.06	29.4	1.30	0.94	0.21	25.49	7.28	BC	b	10	
85S838FG05	07° 29.06'S	157° 31.09'W	5.263	(P I) f l	49	27	24				0.68	E.Sp	2.10	25.6	1.26	0.93	0.22	26.25	7.49	BC	b	20	
85S838FG06	07° 29.05'S	157° 29.16'W	5.210	(P I) f l	72	28					0.79	E.Sp	2.11	25.5	1.31	0.92	0.22	25.50	7.37	BC	ds	0	
(85S13) Average					58	28	16				0.70	E.Sp	2.09	26.7	1.29	0.93	0.22	25.74	7.38				
85S939SC01	07° 59.82'S	157° 00.69'W	5.374	(P I) f l	32	65	3				5.56	Pt.M	2.02	25.0	0.62	0.38	0.36	19.07	12.85	BC	d2	0	
85S939FG02	07° 58.94'S	157° 01.16'W	5.352	(P I) f l	13	45	42				1.34	E.M	1.98	25.3	0.58	0.32	0.25	12.53	9.40	BC	d2	0	
85S939FG03	07° 58.87'S	156° 59.25'W	5.377	(P I) f l	43	57					5.68	E.Sp	2.08	25.2	0.73	0.45	0.29	17.78	10.87	BC	d2	0	
(85S14) Average					35	59	6				4.19	E.Pt	2.04	25.1	0.67	0.40	0.31	17.79	11.59				
85S938FG04	08° 29.90'S	157° 30.03'W	5.319	(P I) f l	91	9					0.60	Sp.E	2.09	27.3	0.55	0.36	0.29	13.04	12.26	BC	c	0	
85S938FG05	08° 28.88'S	157° 31.08'W	5.310	(P I) f l	61	32	7				3.38	Sp.Pl	2.09	25.6	0.51	0.30	0.33	14.54	13.31	BC	c	0	
85S938FG06	08° 28.81'S	157° 29.12'W	5.330	(P I) f l	51	44	5				4.18	E.Sp	2.07	22.1	0.48	0.31	0.32	14.36	13.03	BC	c	0	
(85S15) Average					58	36	5				2.72	Sp.E	2.08	23.9	0.50	0.31	0.32	14.34	13.09				
85S939FG04	08° 29.93'S	156° 29.90'W	5.462	(P I) f l	100						0.05	Sp.E	0.00	25.0	1.21	0.87	0.20	21.26	6.62	BC	b	30	
85S939FG05	08° 28.88'S	156° 30.84'W	5.465	(P I) f l	100						0.05	E.Sp	—	—	—	—	—	—	—	BC	b	20	
85S939FG06	08° 28.77'S	156° 28.86'W	5.427	(P I) f l	100						0.04	Sp.E	—	—	—	—	—	—	—	BC	b	10	
(85S16) Average					100						0.05	Sp.E	0.00	25.0	1.21	0.87	0.20	21.26	6.62				
85S839FG04	07° 30.12'S	156° 29.94'W	4.841	(P I) f l							0.00	—	—	—	—	—	—	—	—	CC	ds	0	
85S839FG05	07° 29.24'S	156° 31.02'W	4.544	(P I) m t							0.00	—	—	—	—	—	—	—	—	-	ds	0	
85S839FG06	07° 29.33'S	156° 29.09'W	4.882	(P I) f l	83	17					0.09	Pl.Sp	—	—	—	—	—	—	—	CSC	b	20	
(85S17) Average					83	17					0.03	Pl.Sp	—	—	—	—	—	—	—				
85S940FG01	08° 00.02'S	155° 59.95'W	5.359	(P I) f l	100						0.09	Sp.E	—	—	—	—	—	—	—	BC	b	30	
85S940FG02	07° 59.09'S	156° 00.98'W	5.383	(P I) f l	55	45					0.24	E.Sp	—	—	—	—	—	—	—	BC	b	30	
85S940FG03	07° 59.11'S	155° 59.08'W	5.336	(P I) f l	59	41					0.45	Sp.E	2.08	28.7	1.26	0.98	0.20	25.42	7.02	BC	b	30	
(85S18) Average					63	38					0.26	Sp.E	2.08	29.7	1.26	0.98	0.20	25.42	7.02				

* T.P.L. : Transparent Layer

Data file around the Cook Islands

(No. 4)

Sample No (Station)	Location				Manganese Nodules															Geology			Remarks
					Size distribution (%)						Abun-dance	Shape	S.G. wet	H2O	XRF Analyses (%)					Sediment	T.P.L.*		
	Latitude	Longitude	Depth (m)	Topography	0-2 cm	2-4 cm	4-6 cm	6-8 cm	8-16 cm	16- cm	(Kg/m2)			(%)	Ni	Cu	Co	Mn	Fe		type	thick (m)	
85S840FC01	07° 00.04'S	156° 00.02'W	5.229	(P I) f f	100						0.33	Ot.E	2.00	16.3	0.44	0.34	0.12	6.17	6.46	BC	b	20	
85S840FC02	06° 59.21'S	156° 01.08'W	5.182	(P I) f f	87	13					1.38	Ot.E	2.09	19.2	0.58	0.40	0.17	8.49	9.21	BC	b	10	
85S840FC03	06° 59.21'S	155° 59.22'W	5.186	(P I) f f	100						0.03	Ot.Sp	—	—	—	—	—	—	—	BC	b	10	
(85519) Average					90	10					0.58	Ot.E	2.07	18.8	0.55	0.39	0.16	8.03	8.68				
85S739FC01	06° 29.98'S	156° 30.03'W	5.231	(P I) f f	43	57					3.28	E.Pt	2.03	24.0	1.02	0.60	0.20	17.86	9.16	BC	b	10	
85S739FC02	06° 29.01'S	156° 31.03'W	5.218	(P I) f f	49	45	6				4.54	E.Pt	2.09	24.5	1.07	0.69	0.21	20.65	7.90	BC	d2	0	
85S739FC03	06° 29.06'S	156° 29.19'W	5.195	(P I) f f	37	38	25				4.24	E.Pt	2.07	29.0	1.03	0.72	0.27	23.45	8.96	BC	d2	0	
(85520) Average					43	46	11				4.02	E.Pt	2.07	25.9	1.04	0.68	0.23	20.82	8.61				
85S938FC07	08° 30.14'S	157° 59.93'W	4.895	(P I) h i							0.00	—	—	—	—	—	—	—	—	—	ds	0	
85S938FC08	08° 29.26'S	158° 00.94'W	5.046	(P I) h i	11	3	9		77		1.38	Pl.E	2.12	25.9	0.37	0.24	0.30	14.45	13.04	CC	ds	0	
85S938FC09	08° 29.22'S	157° 59.01'W	4.910	(P I) h i	73	27					0.20	Pl.Ot	—	—	—	—	—	—	—	CC /FO	ds	0	
(85521) Average					19	6	8		67		0.53	Pl.E	2.12	25.9	0.37	0.24	0.30	14.45	13.04				
85S937FC07	08° 14.99'S	158° 14.82'W	5.583	(P I) f f	80	20					2.71	Sp.E	2.06	25.8	0.56	0.33	0.32	15.74	12.95	BC	c	0	
85S937FC08	08° 14.07'S	158° 15.75'W	5.582	(P I) f f	73	27					3.56	E.Sp	2.02	25.1	0.54	0.32	0.33	16.24	13.25	BC	c	0	
85S937FC09	08° 14.05'S	158° 13.79'W	5.576	(P I) f f	67	33					3.91	E.Sp	2.01	29.8	0.54	0.32	0.34	16.37	13.35	BC	c	0	
(85522) Average					73	27					3.39	E.Sp	2.03	27.1	0.54	0.32	0.33	16.15	13.21				
85S936FC04	08° 00.17'S	159° 29.52'W	5.260	(M o) t a	40	60					3.58	E.Pt	1.97	29.8	0.64	0.35	0.36	17.86	14.17	BC	b	5	
85S936FC05	07° 59.16'S	159° 30.40'W	5.152	(M o) t a	10	62	19	5	4		18.63	E.Pt	1.87	30.0	0.40	0.26	0.39	15.69	16.21	SCC	ds	0	
85S936FC06	07° 59.10'S	159° 28.34'W	5.256	(M o) t a	59	41					1.32	E.Sp	2.06	29.2	0.69	0.40	0.32	17.56	12.50	BC	b	20	
(85523) Average					17	61	15	4	3		7.84	E.Pt	1.97	30.0	0.45	0.28	0.38	16.12	15.69				
85S936FC07	08° 14.95'S	159° 14.88'W	5.778	(M o) h o							0.00	—	—	—	—	—	—	—	—	BC	c	0	
85S936FC08	08° 14.01'S	159° 15.89'W	5.657	(M o) h o	17	75	8				10.68	Pl.M	1.91	29.1	0.16	0.15	0.16	2.23	15.30	BC	ds	0	
85S936FC09	08° 13.96'S	159° 14.00'W	5.770	(M o) h o	100						0.02	Ot.E	—	—	—	—	—	—	—	BC	c	0	
(85524) Average					17	75	8				3.56	Pl.M	1.91	29.1	0.16	0.15	0.16	2.23	15.30				

* T.P.L : Transparent Layer

Data file around the Cook Islands

(No 5)

Sample No. (Station)	Location: Latitude	Longitude	Depth (m)	Topography	Manganese Nodules: Size distribution (%) 0-2 cm	2-4 cm	4-6 cm	6-8 cm	8-16 cm	16- cm	Abundance (Kg/m2)	Shape	S.G. wet	H2O (%)	XRF Analyses (%) Ni	Cu	Co	Mn	Fe	Geology: Sediment	T.P.L.* type	thick (m)	Remarks
85S937FG10	08° 14.96'S	158° 44.69'W	5.604	(P l) f l	82	18					0.50	Sp.E	2.04	28.6	1.08	0.77	0.22	21.53	9.13	BC	c	0	
85S937FG11	08° 13.96'S	159° 45.58'W	5.596	(P l) f l	58		42				0.85	M.Sp	2.24	18.3	0.66	0.48	0.14	11.94	4.98	BC	c	0	
85S937FG12	08° 13.88'S	158° 43.49'W	5.613	(P l) f l	32	42			26		2.00	Sp.M	0.00	30.9	0.74	0.50	0.26	16.95	10.48	BC	c	0	
(85525) Average					46	28	11		16		1.12	Sp.M	2.17	27.6	0.77	0.53	0.22	16.21	8.73				
85S937FG13	08° 30.07'S	159° 00.05'W	5.524	(M o) f l	100						0.05	Sp.Ot	0.00	25.9	0.76	0.51	0.26	16.31	10.78	BC	c	0	
85S937FG14	08° 29.01'S	159° 01.03'W	5.515	(M o) f l	100						0.12	Sp.E	—	—	—	—	—	—	—	BC	c	0	
85S937FG15	08° 29.00'S	158° 59.12'W	5.538	(M o) f l	100						0.04	Sp.E	—	—	—	—	—	—	—	BC	c	0	
(85526) Average					100						0.07	Sp.E	0.00	25.9	0.76	0.51	0.26	16.31	10.78				
85S836FC04	07° 44.96'S	159° 14.91'W	5.550	(M o) f l	4	37	24	23	12		20.82	E.Pt	1.87	29.5	0.31	0.20	0.48	18.40	16.44	BC	b	10	
85S836FC05	07° 43.96'S	159° 15.88'W	5.525	(M o) f l	2	12	16	22	48		31.87	El.E	1.92	29.5	0.27	0.15	0.51	18.39	16.27	BC	b	5	
85S836FC06	07° 43.78'S	159° 13.90'W	5.634	(M o) f l	3	70	21	6			13.88	Pt.E	1.91	32.0	0.48	0.26	0.40	14.70	14.70	BC	b	5	
(85527) Average					3	32	20	19	27		22.22	E.El	1.94	30.0	0.32	0.19	0.48	17.64	16.00				
85S837FG07	07° 29.98'S	158° 59.93'W	5.392	(P l) f l	77	23					1.02	Sp.E	2.05	28.2	1.17	0.88	0.23	23.52	8.49	BC	b	10	
85S837FG08	07° 29.05'S	159° 00.96'W	5.395	(P l) f l	43	57					0.32	E.Sp	—	—	—	—	—	—	—	BC	b	10	
85S837FG09	07° 28.97'S	158° 59.05'W	5.398	(P l) f l	83	17					0.59	E.Sp	2.00	20.5	1.26	0.90	0.23	24.31	8.23	BC	c	0	
(85528) Average					73	27					0.64	Sp.E	2.03	25.4	1.21	0.87	0.23	23.83	8.39				
85S937FG16	07° 59.99'S	158° 29.99'W	5.535	(P l) f l	57	43					1.26	Sp.E	1.93	26.4	0.98	0.65	0.23	19.54	9.79	BC	c	0	
85S937FG17	07° 59.08'S	158° 30.96'W	5.538	(P l) f l	64	36					1.27	E.Sp	2.01	25.2	1.00	0.70	0.22	19.77	8.44	BC	c	0	
85S937FG18	07° 58.98'S	158° 29.05'W	5.521	(P l) f l	87	13					1.20	Sp.E	2.09	25.8	1.09	0.76	0.23	21.25	8.56	BC	c	0	
(85529) Average					69	31					1.24	Sp.E	2.01	25.8	1.02	0.70	0.23	20.17	8.93				
85S837FG10	07° 44.87'S	158° 45.07'W	5.559	(P l) f l	54	46					0.77	E.Sp	2.17	30.3	0.99	0.67	0.23	19.69	9.58	BC	c	0	
85S837FG11	07° 43.94'S	158° 46.12'W	5.529	(P l) f l	71	29					0.26	Sp.E	—	—	—	—	—	—	—	BC	b	20	
85S837FG12	07° 43.92'S	158° 44.20'W	5.553	(P l) f l	79	21					0.22	Sp.E	—	—	—	—	—	—	—	BC	b	20	
(85530) Average					62	38					0.42	Sp.E	2.17	30.3	0.99	0.67	0.23	19.69	9.58				

* T.P.L : Transparent Layer

Data file around the Cook Islands

(No. 5)

Sample No. (Station)	Location				Manganese Nodules: Size distribution (%)						Abundance (Kg/m2)	Shape	S.G. wet	H2O (%)	XRF Analyses (%)					Geology			Remarks
	Latitude	Longitude	Depth (m)	Topography	0-2 cm	2-4 cm	4-6 cm	6-8 cm	8-18 cm	18- cm					Ni	Cu	Co	Mn	Fe	Sediment	T.P.L.* type	T.P.L.* thick (m)	
85S838FG07	07° 29.79'S	157° 59.85'W	5.416	(Pl) fl	15	85					1.02	E.Pt	2.07	25.0	0.72	0.48	0.28	18.80	11.30	BC	ds	0	
85S838FG08	07° 28.84'S	158° 00.84'W	5.403	(Pl) fl							0.00	—	—	—	—	—	—	—	—	-	ds	0	
85S838FG09	07° 28.66'S	157° 58.88'W	5.493	(Pl) fl	81	19					0.12	E.Sp	—	—	—	—	—	—	—	BC	el	10	
(85S31) Average					22	78					0.88	E.Pt	2.07	25.0	0.72	0.48	0.28	18.80	11.30				
85S837FG13	07° 45.12'S	158° 14.96'W	5.440	(Pl) fl	56	33	11				3.19	Sp.E	1.98	28.0	1.03	0.71	0.26	22.42	10.06	BC	el	10	
85S837FG14	07° 44.08'S	158° 15.90'W	5.428	(Pl) fl	46	54					2.11	E.Sp	1.99	31.0	1.03	0.73	0.26	23.56	10.12	BC	el	10	
85S837FG15	07° 44.01'S	158° 13.98'W	5.439	(Pl) fl	65	17	8	10			2.73	Sp.E	2.06	24.5	0.87	0.56	0.30	21.54	11.57	BC	d2	0	
(85S32) Average					56	33	7	3			2.68	Sp.E	2.01	27.6	0.97	0.66	0.27	22.40	10.61				
85S837FG16	07° 15.03'S	158° 14.99'W	5.339	(Pl) fl	100						0.21	E.Sp	—	—	—	—	—	—	—	BC	el	10	
85S837FG17	07° 14.12'S	158° 16.02'W	5.320	(Pl) fl	70	30					0.15	E.Sp	—	—	—	—	—	—	—	BC	el	10	
85S837FG18	07° 14.06'S	158° 14.13'W	5.312	(Pl) fl	26	62		12			1.94	M.Pt	2.05	28.6	0.80	0.46	0.25	15.41	10.77	BC	ds	0	
(85S33) Average					36	54		10			0.77	M.Pt	2.05	28.6	0.80	0.46	0.25	15.41	10.77				
85S837FG19	07° 14.77'S	158° 45.04'W	5.304	(Pl) fl	68	32					0.38	E.Sp	2.13	28.1	1.25	0.84	0.21	22.83	7.95	BC	b	20	
85S837FG20	07° 13.85'S	158° 46.02'W	5.332	(Pl) fl	92	8					0.57	Sp.E	2.06	27.5	1.24	0.83	0.22	23.23	7.94	BC	b	10	
85S837FG21	07° 13.75'S	158° 44.10'W	5.328	(Pl) fl	67	19	14				0.94	Sp.E	2.05	30.0	1.34	0.86	0.21	24.04	7.53	BC	b	10	
(85S34) Average					75	18	7				0.63	Sp.E	2.07	28.9	1.29	0.85	0.21	23.55	7.74				
85S737FG04	06° 30.16'S	158° 59.86'W	5.259	(Pl) fl	6	39	55				1.04	E.Ef	2.02	28.2	1.06	0.97	0.17	27.93	7.09	BC	b	40	
85S737FG05	06° 29.29'S	159° 00.90'W	5.283	(Pl) fl	3	97					0.66	E	2.08	28.3	1.00	0.93	0.16	25.32	6.55	BC	b	50	
85S737FG06	06° 29.26'S	158° 58.95'W	5.261	(Pl) fl	10	90					0.37	E.Sp	0.00	23.3	1.07	0.98	0.18	28.56	7.04	BC	b	40	
(85S35) Average					6	67	28				0.69	E.Ef	2.04	26.4	1.04	0.96	0.17	27.24	6.92				
85S736FG04	06° 45.04'S	159° 15.10'W	5.212	(Mo) hi	56	44					3.80	E.M	2.03	28.8	0.64	0.40	0.32	17.06	11.90	DC	ds	0	
85S736FG05	06° 44.20'S	159° 16.20'W	5.318	(Mo) hi	49	51					1.39	E.M	2.11	24.0	0.93	0.59	0.21	17.29	8.96	BC	ds	0	
85S736FG06	06° 44.33'S	159° 14.40'W	5.292	(Mo) hi	36	45	19				3.72	E.M	2.27	19.8	0.43	0.29	0.23	10.56	10.30	BC	ds	0	
(85S36) Average					47	45	8				2.97	E.M	2.14	24.3	0.59	0.38	0.26	14.22	10.73				

* T.P.L : Transparent Layer

Data file around the Cook Islands

(No. 7)

Sample No (Station)	Location: Latitude	Location: Longitude	Location: Depth (m)	Location: Topography	Size distribution (%): 0-2 cm	2-4 cm	4-6 cm	6-8 cm	8-16 cm	16- cm	Abundance (Kg/m2)	Shape	S.G wet	H2O (%)	XRF Analyses (%): Ni	Cu	Co	Mn	Fe	Geology: Sediment	T.P.L.* type	T.P.L.* thick (m)	Remarks
85S836FG07	06° 59.97'S	159° 30.04'W	5.274	(Mo) mi		11		89			2.25	Sp.Ot	1.96	29.8	0.18	0.09	0.52	18.02	18.42	-	d2	0	
85S836FG08	06° 59.06'S	159° 31.13'W	5.331	(Mo) mi	17	51	20	12			6.22	M.Pt	1.97	28.4	0.60	0.36	0.38	18.96	13.30	BC	b	10	
85S836FG09	06° 59.08'S	159° 29.29'W	5.237	(Mo) mi	14	64	22				12.15	Pt.E	2.02	28.5	0.44	0.28	0.41	19.20	15.72	BC	b	10	
(85S37) Average					13	54	19	13			6.87	Pt.M	2.00	28.6	0.46	0.28	0.41	19.00	15.28				
85S836FG10	07° 14.85'S	159° 15.15'W	5.372	(Mo) ta							0.00	—	—	—	—	—	—	—	—	-	ds	0	
85S836FG11	07° 13.88'S	159° 16.06'W	5.310	(Mo) ta	42	58					0.48	E.Sp	2.00	30.6	0.87	0.56	0.31	21.38	11.29	BC	el	10	
85S836FG12	07° 13.78'S	159° 14.33'W	5.431	(Mo) ta	82	18					0.55	E.Ot	2.04	20.9	0.44	0.29	0.17	7.20	8.75	BC	c	0	
(85S38) Average					63	37					0.34	E.Sp	2.02	25.4	0.63	0.41	0.23	13.35	9.85				

* T.P.L : Transparent Layer

(No.8)

Wind direction (in 1985)

direct / Month	CALM	N	NNE	NE	ENE	E	ESE	SE	SSE	S	SSW	SW	WSW	W	WNW	NW	NNW	total
Apr.																		
May																		
June																		
July																		
Aug.																		
Sept.																		
Oct.	23 4.16	5 0.90	14 2.53	88 15.91	103 18.63	218 39.42	49 8.86	17 3.07	1 0.18	0 0	0 0	3 0.54	2 0.36	13 2.35	1 0.18	9 1.63	7 1.27	553
Nov.																		
Dec.																		

Measurement: every hours

(No.9)

Wind velocity (in 1985)

Velocity: m/sec.

velicity / month	0	1	2	3	4	5	6	7	8	9	10	11	12	13	14	15	total
Apr.																	
May																	
June																	
July																	
Aug.																	
Sept.																	
Oct.	22 3.98	0 0	10 1.81	22 3.98	26 4.70	56 10.13	72 13.02	51 9.22	103 18.63	75 13.56	15 2.71	0 0	0 0	0 0	0 0	0 0	553
Nov.																	
Dec.																	

Measurement: every hours

(No. 10)

Weather (in 1985)

weather / month	Blue Sky	Cloudy	Rainy	Total	Precipitation
Apr.					
May					
June					
July					
Aug.					
Sept.					
Oct.	22 95.65	1 4.35	0 0	23	7
Nov.					
Dec.					

(No. 11)

Atmospheric pressure (in 1985)

Atm. press.: mb

Atm. Press. / Month	1007.1 ~ 100.80	1008.1 ~ 1009.0	1009.1 ~ 1010.1	1010.1 ~ 1011.0	1011.1 ~ 1012.0	1012.1 ~ 1013.0	1031.1 ~ 1014.0	1014.1 ~ 1015.0	1015.1 ~ 1016.0	total
Apr.										
May										
June										
July										
Aug.										
Sept.										
Oct.	7 1.27	41 7.41	115 20.80	135 24.41	129 23.33	81 14.65	34 6.15	10 1.81	1 0.18	553
Nov.										
Dec.										

Measurement: every hours

(No. 12)

Swell-direction (in 1985)

direct / month	N	NNE	NE	ENE	E	ESE	SE	SSE	S	SSW	SW	WSW	W	WNW	NW	NNW	Indis-tinctive	total
Apr.																		
May																		
June																		
July																		
Aug.																		
Sept.																		
Oct.	0 0	0 0	4 2.88	23 16.55	20 14.39	15 10.79	3 2.16	7 5.04	0 0	0 0	0 0	0 0	0 0	0 0	0 0	0 0	67 48.20	139
Nov.																		
Dec.																		

Measurement: every 4 hours

(No. 13)

Swell-Cycle (in 1985)

Swell cycle / month	5	6	7	8	9	10	11	12	13	14	15	none	Total
Apr.													
May													
June													
July													
Aug.													
Sept.													
Oct.	0 0	28 20.14	44 31.65	0 0	0 0	0 0	0 0	0 0	0 0	0 0	0 0	67 48.20	139
Nov.													
Dec.													

Measurement: every 4 hours

(No. 14)

Swell-hight (in 1985)

Wave-hight: m

Swell-hight / month	1	2	3	4	5	none	Total
Apr.							
May							
June							
July							
Aug.							
Sept.							
Oct.	0 0	16 11.51	5.6 40.29	0 0	0 0	67 48.20	139
Nov.							
Dec.							

Measurement: every 4 hours

Cloudness (in 1985)

month	0	1	2	3	4	5	6	7	8	9	total
Apr.											
May											
June											
July											
Aug.											
Sept.											
Oct.	0 0	46 8.32	137 24.77	236 42.68	56 10.13	26 4.70	28 5.06	20 3.62	4 0.72	0 0	553
Nov.											
Dec.											

Measurement: every hour